AD_____

Award Number: DAMD17-00-1-0529

TITLE: Studies of Role of Cathepsin K and Inhibitory Effects of Bisphosphonates in Prostate Cancer Bone Metastasis

PRINCIPAL INVESTIGATOR: Eva Corey, Ph.D.

CONTRACTING ORGANIZATION: University of Washington
Seattle, Washington 98105

REPORT DATE: August 2003

TYPE OF REPORT: Annual

PREPARED FOR: U.S. Army Medical Research and Materiel Command
Fort Detrick, Maryland 21702-5012

REPORT DOCUMENTATION PAGE

Form Approved
OMB No. 074-0188

1. AGENCY USE ONLY (Leave blank)	2. REPORT DATE	3. REPORT TYPE AND DATES COVERED
	August 2003	Annual (1 Aug 2002 - 31 Jul 2003)

4. TITLE AND SUBTITLE
Studies of Role of Cathepsin K and Inhibitory Effects of Bisphosphonates in Prostate Cancer Bone Metastasis

5. FUNDING NUMBERS
DAMD17-00-1-0529

6. AUTHOR(S)
Eva Corey, Ph.D.

7. PERFORMING ORGANIZATION NAME(S) AND ADDRESS(ES)
University of Washington
Seattle, Washington 98105

E-Mail: ecorey@u.washington.edu

8. PERFORMING ORGANIZATION REPORT NUMBER

9. SPONSORING / MONITORING AGENCY NAME(S) AND ADDRESS(ES)
U.S. Army Medical Research and Materiel Command
Fort Detrick, Maryland 21702-5012

10. SPONSORING / MONITORING AGENCY REPORT NUMBER

11. SUPPLEMENTARY NOTES

12a. DISTRIBUTION / AVAILABILITY STATEMENT
Approved for Public Release; Distribution Unlimited

12b. DISTRIBUTION CODE

13. ABSTRACT (Maximum 200 Words)

Prostate cancer (CaP) is often associated with bone metastases, which cause much of the morbidity associated with CaP. CaP bone metastases exhibit increases in both bone formationand resorption. In studies under this award, we have investigated the expression and activity of Cathepsin K (Cat K), an enzyme involved in bone lysis in CaP in vitro and in vivo. The Cat K message and protein were detected in CaP cell lines, primary Cap samples, and metastatic samples. Expression of Cat K in bone metastases was significantly higher than in primary CaP. Cat K enzymatic activity was detected in CaP cell lines. ZA decreased the proliferation of CaP cells and caused apoptosis of CaP cells in vitro. In vivo, growth of osteoblastic and osteolytic metastases of CaP was significantly inhibited; however, growth of subcutaneous tumors was unaffected by ZA, indicating that he growth-inhibition effects were directly related to the interactions between ZA and bone, and/or CaP metastases in bone. Treatment of C4-2 mixed CaP bone metastases resulted in decreased numbers of osteoclasts, but the effects on tumor volume were method-dependent. Evaluation of the effects of ZA on bone seeding, using cardiac injection model, is ongoing.

14. SUBJECT TERMS
Prostate cancer, bone metastases, Cathepsin K, Bisphosphonates

15. NUMBER OF PAGES
62

16. PRICE CODE

17. SECURITY CLASSIFICATION OF REPORT	18. SECURITY CLASSIFICATION OF THIS PAGE	19. SECURITY CLASSIFICATION OF ABSTRACT	20. LIMITATION OF ABSTRACT
Unclassified	Unclassified	Unclassified	Unlimited

Table of Contents

INTRODUCTION

This report describes our investigation of the effects of two molecules on prostate-cancer (CaP) bone metastases: Cathepsin K (CatK), an enzyme implicated in degradation of bone leading to establishment and/or growth of the metastases, and zoledronic acid (ZA), a new-generation bisphophonate that is a strong inhibitor of osteolysis. Our first hypothesis holds that CatK expressed by CaP is involved in bone extracellular matrix degradation, and that this degradation promotes tumor establishment and growth. The work performed under this task has been directed toward testing of this hypothesis *in vitro.* At this point we have sound evidence regarding the involvement of CatK in CaP (especially with regard to degradation of collagen I, a component of bone extracellular matrix) and a paper has been published in *J. Bone Min Res*[1] (attached). However we have not succeeded in abolishing the CatK message in CaP cells, and as a result the *in vivo* studies have not been performed. Our second hypothesis holds that bisphophonates such as ZA act to slow or reverse the effects of CaP not only by inhibiting lysis of bone (an effect likely to be mediated largely by osteoclasts, although CaP cells may be involved as well). We have been able to demonstrate direct effects of ZA *in vitro*, including stimulation of apoptosis of CaP cells. Our *in vivo* results in osteoblastic and osteolytic models also showed decreased tumor growth upon ZA administration. These results are described in our publication in *Clin Cancer Res*[2] (attached). We have also performed experiments in a mixed (osteoblastic/osteolytic) C4-2 CaP model, where the results are inconsistent, depending on analysis. Finally, we have begun studies to determine whether ZA affects establishment and growth of bone and soft tissue metastases.

Background

Bone is a very common site of prostate cancer (CaP) metastases [3,4], and bone metastases are responsible for most of the morbidity associated with this disease. In contrast to bone metastases of breast cancer and myeloma, which are mainly osteolytic, a high percentage of CaP metastases exhibit the radiographic appearance of osteoblastic lesions[5]. Histomorphometric studies of CaP bone metastases have shown that some of the sclerotic lesions are actually mixed in nature, with increased activities of both osteoblasts and osteoclasts[6,7]. Roland has introduced the hypothesis that every primary or metastatic cancer in bone begins with osteolysis[8]. A number of studies have shown that patients with advanced CaP exhibit elevated levels of osteolytic bone resorption markers in urine and blood[9,10]. The preponderance of evidence indicates that osteolysis is present in CaP bone metastasis even when the overall character appears to be osteoblastic. It follows that the use of compounds inhibiting osteolysis could be beneficial to patients with advanced CaP. Zoledronic acid (ZA) is a new-generation BP with a side chain containing an imidazole ring, and is one of the most potent BPs [11,12]. Berenson *et al.* reported reduction of rates of skeletal events in metastatic patients by ZA[13]. Recently it has been published that ZA had beneficial effects when used to treat patients with advanced prostate cancer.

Various studies suggest that cysteine proteases participate in bone degradation [14-18]. CatK, a cysteine protease expressed by osteoclasts, appears to be essential for osteoclast-mediated collagen degradation [19]. Active CatK was detected in osteoclasts close to the bone surface, in contrast to osteoclasts further from the surface [20], again suggesting that CatK is an important player in bone lysis. It has also been shown that CatK is expressed in several other normal cell types [21,22], and in breast cancer, but the expression was lower that in osteoclasts [23]. Tumor cells

were frequently found adjacent to resorbed bone margins without evidence of resorbing osteoclast [24-26], and there is some evidence that breast cancer cells directly resorb bone [25,27,28]. We and others have detected CatK messages in normal prostate, and we have extended these findings to detection of the CatK message in CaP tissues and in all CaP cancer cell lines. In a preliminary study, Brawer *et al.* showed that the N-telopeptide of collagen [29,30], a CatK-generated cleavage product, is present in urine of CaP patients with bone metastases. These data confirm that osteolytic activity attributable to CatK takes place in CaP bone metastases.

HYPOTHESES

We have two primary hypotheses:

1. We hypothesize that CatK, expressed by CaP cells, promotes bone resorption, thereby enabling the establishment and growth of CaP cells in the bone environment. The mechanisms of action of CatK in this system will be shown to involve both osteoclast-like pitting of bone and proteolytic release of growth factors present in bone ECM.
2. We hypothesize that BP, in addition to their effects on bone cells, affect CaP cells directly *via* apoptosis and inhibition of invasiveness and migration, and thus inhibit establishment of CaP cells in the bone environment.

STATEMENT OF WORK

Task 1. Examination of the Role of Cathepsin K Expressed by LNCaP and PC-3 Cells in Collagen Degradation and Attachment of CaP Cells to Bone in an *in vitro* Model Using Osteogenic Disks (0-24 months).

- Examination of collagen degradation by CaP cells. Co-culture experiments to study effects of CaP cells on osteoclast degradation of collagen (months 0-8).
- Immunohistochemical determination of presence of pro-form and mature Cathepsin K in prostate cells, and biochemical determination of Cathepsin K activity in these cells (months 0-12).
- Determination of the pitting activity of CaP cells alone or in combination with osteoclasts on osteogenic disks (months 6-12).
- Transfection of CaP cells expressing Cathepsin K with anti-Cathepsin K ribozyme to abolish expression of the protein (months 6-18).
- Characterization of transfected cells in *in vitro* setting (proliferation, migration, invasiveness, collagen degradation, and pitting activity on osteogenic disks (months 18-24)).

Tasks 2. Determination as to whether Bisphosphonates (BP) Affect CaP Cells Directly (0-18 months).

- Determination of effects of BP on proliferation, migration, and invasiveness of CaP cells (months 0-12).
- Determination of effects of BP on apoptosis of CaP cells (months 0-12).
- Determination of effects of BP on collagen degradation and/or pitting activity of CaP cells (months 12-18).

Task 3. Examination of Roles of Cathepsin K and BP on CaP Metastasis in *in vivo* Models (18-36 months).

- Determination of *in vivo* effects of CaP cells transfected with anti-Cathepsin K ribozyme when injected into tibia (months 24-36).
- Determination of effects of BP on LNCaP, LuCaP 23, and PC-3 CaP xenografts growth in tibia (months 18-36).
- Determination of effects of BP on seeding of PC-3 following cardiac injection (months 24-36).

BODY

Task 1. Examination of the Role of Cathepsin K Expressed by LNCaP and PC-3 Cells in Collagen Degradation and Attachment of CaP Cells to Bone in an *in vitro* Model Using Osteogenic Disks.

- **Examination of collagen degradation by CaP cells. Co-culture experiments to study effects of CaP cells on osteoclast degradation of collagen (months 0-8).**
- **Immunohistochemical determination of presence of pro-form and mature Cathepsin K in prostate cells, and biochemical determination of Cathepsin K activity in these cells (months 0-12).**
- **Determination of the pitting activity of CaP cells alone or in combination with osteoclasts on osteogenic disks (months 6-12).**

These tasks were completed during years 01 and 02 of this award. Results were published in *Journal of Bone and Mineral Research 2003* [1] (attached). We were unable to detect any pitting activity of dentine wafers associated with CaP cells. We then hypothesized that bone resorption requires the low pH produced by osteoclasts in lacunae in which protons and proteases are both secreted. Therefore, we evaluated further whether CaP-expressed CatK can resorb non-mineralized bone extracellular matrix, in particular type I collagen. Using radiolabelled collagen I, we detected release of collagen fragments using CaP cells, as well as osteoclasts (see Figure 5 of reference (1), attached). We have also shown that levels of collagen-degradation product NT, generated by CatK cleavage, are increased in sera of patients with bone metastases (see Figure 6 of reference (1), attached). Augmented NTx levels are generally associated with increased osteoclastic bone resorption activity due to CatK expressed by these cells, yet we observed osteoclasts in only 3/14 samples of advanced CaP bone metastases. Although we sample 20 bone sites per patient, it is possible that we missed areas with extensive bone resorption and osteoclasts. Alternatively, the increased NTx levels may in part be due to the breakdown of type I collagen by cells other than osteoclasts, such as the CaP cells expressing CatK. While these data do not demonstrate a direct role of CaP-expressed CatK in matrix degradation, they support the hypothesis that CaP-expressed CatK is involved in collagen degradation. Detailed results are presented in the attached manuscript. In the same publication we have also presented data on detection of CatK messages and protein in human samples (Table 1 and Figures 2 and 3 of [1]).

- **Transfection of CaP cells expressing CatK with anti-Cathepsin K ribozyme to abolish expression of the protein.**

During year 01 and 02 we devoted large efforts to generate anti-CatK ribozyme. Unfortunately, as reported last year we did not succeed in constructing a ribozyme capable of abolishing expression of CatK in CaP cells. Based on the recommendation of reviewers of the second year report and new literature reports, we have decided to use siRNA technology to abolish CatK expression in CaP cells. It has been established that short (under 30nt) strands of dsRNA will act to silence target gene sequences in mammalian models using an enzyme complex called the RISC Complex. Although the RISC Complex has escaped definition thus far, the reaction it produces has been adapted for a variety of research uses. siRNA have been shown to silence genes in all types of biological models including human biology. We have used an siRNA-specific primer design tool (www.Ambion.com) to select sequences for anti-CatK siRNA. We chose 4 target sequences positioned throughout the CatK open reading frame sequence (see Table 1). siRNAs were synthesized using Ambion's *Silencer* siRNA:

Position of NM_000396	Sense Strand	Antisense Strand
231	5'- AACATCCACCTTGTTGTTATACCTGTCTC -3'	5'- AATATAACAACAAGGTGGATGCCTGTCTC -3'
389	5'- AATACTTTGAGTCCAGTCATCCCTGTCTC -3'	5'- AAGATGACTGGACTCAAAGTACCTGTCTC -3'
490	5'- AAGGAGTAACATATCCTTTCTCCTGTCTC -3'	5'- AAAGAAAGGATATGTTACTCCCCTGTCTC -3'
584	5'- AATAAGAGTTTGCCAGTTTTCCCTGTCTC -3'	5'- AAGAAAACTGGCAAACTCTTACCTGTCTC -3'

Transfection experiments were performed with C4-2B cells. We tested two different transfection agents (Lipofectamine and **xx**), two different concentrtations of siRNA (10 and 25 ng), and two time points after transfection (24 and 48 hours). Evaluation of the results of the transfection was performed using real-time PCR and measuring enzymatic activity. For real-time PCR we selected two sets of primers which were located in CatK open-reading frame and followed the recommendations of Ambion (Table 2).

Gene	Left	Right	Annealing temp for PCR
CTSK (primer set 1)	5'-AGA AGA CCC ACA GGA AGC AA-3'	5'-GCT AAA AGC CCA ACA GGA AC-3'	65c
CTSK (primer set 2)	5'-AAG GGA AAC AAG CAC TGG ATA A-3'	5'-CTT CAA AAA TAG CAC ACC AAC TCC-3'	69c

Real-time analysis was performed using the GeNorm standard normalizing calculation method described by Vandesompele *et. al.* [31]. We have evaluated expression of five "housekeeping genes" (Table 3).

Housekeeping Gene	Left	Right	Optimum PCR temp
PSMB6	5'-GGG TAT GAT GGT AAG GCA GTC C-3'	5'- AGG ATT CAG GCG GGT GGT AAA GT -3'	69
GAPDH 2	5'-TGC ACC ACC AAC TGC TTA GC-3'	5'- GGC ATG GAC TGT GGT CAT GAG -3'	65
HMBS	5'-TGC AAC GGC GGA AGA AAA C-3'	5'- GGC TCC GAT GGT GAA GCC -3'	65
HPRT	5'-TGA CAC TGG CAA AAC AAT GCA-3'	5'- GGT CCT TTT CAC CAG CAA GCT -3'	65
EGP	5'-GCT GGA ATT GTT GTG CTG GTT ATT TC-3'	5'-TGT GTC CAT TTG CTA TTT CCC TTC TTC-3'	69

Proteasome subunit beta type 6 (PSMB6) and Glyceraldehyde 3-phosphate dehydrogenase (GAPDH) were the two most stably represented genes and were chosen to normalize the CatK real-time PCR results.

Unfortunately, none of the siRNA sequences, under any conditions tested, resulted in reduced expression of CatK.

Tasks 2. Determination as to whether Bisphosphonates (BP) affect CaP Cells directly (0-18 months).

- Determination of effects of BP on proliferation, migration, and invasiveness of CaP cells (months 0-12).
- Determination of effects of BP on apoptosis of CaP cells (months 0-12).
- Determination of effects of BP on collagen degradation and/or pitting activity of CaP cells (months 12-18).

Experiments under this Task have been completed in year 02 and were described in detail in the year 01 and 02 reports. They were also published in *Clinl Cancer Res*[32] (see attached reprint).

Task 3. Examination of Roles of Cathepsin K and BP on CaP Metastasis *in Vivo* Models (months 18-36).

- **Determination of *in vivo* effects of CaP cells transfected with anti-Cathepsin K ribozyme when injected into tibia (months 24-36).**

We were not able to perform these experiments, since we did not succeed in abolishing CatK expression in CaP cells. We are now trying to contact Novartis, since they now possess a specific anti-CatK inhibitor.

- **Determination of effects of BP on LNCaP, LuCaP 23, and PC-3 CaP xenograft growth in tibia (months 18-36).**

In the year 02 progress report we provided details on effects of ZA on PC-3 bone metastasis (PC-3 cells are responsive to ZA *in vitro* and yield lytic bone metastases), and LuCaP 23.1 bone metastasis (LucaP 23.1 cells do not grow *in vitro* but give rise to osteoblastic bone metastases [33]). These studies have been published [32] (reprint is attached). In year 02 and 03 we have extended these studies to evaluation of the effects of ZA on C4-2 bone metastasis. C4-2 is a subline of LNCaP which exhibits a 100% take rate in tibia and more consistent growth characteristics than the parental line. The first step prior to these studies was the detailed characterization of C4-2 bone metastases. This was done with partial support of this award and additional funding. A manuscript summarizing the results of this study has been accepted for publication in *J Bone Miner Res (*manuscript is attached). Briefly, C4-2 cells exhibited a high take rate (100%) and a consistent growth rate in the intra-tibial injections. C4-2 tumors were detectable after 3 weeks in all animals by serum PSA levels, and at that time %TuV/TV was ~54% as determined by histomorphometric analysis. Interestingly, when we examined effects of C4-2 cells on bone at an early time point, 3 weeks after injection of C4-2 cells, we detected a decrease of only ~10% in BMD, which did not reach significance, and there were no significant changes in %BV/TV. We hypothesize that large numbers of tumor cells are required to dysregulate the bone-remodelling equilibrium or that the perturbations require more time to be observable. Longer exposure of bone to the C4-2 cells and increased %TuV/TV resulted in a significant decrease in BMD and in %BV/TV. These results are in agreement with results previously reported with C4-2B cells[34]. Serum PSA levels rose consistently in the intact animals from week 2 until the end of the experiment, closely tracking the tumor volume. Androgen suppression caused a decrease in

serum PSA levels, with a nadir at 2 weeks post-castration, after which serum PSA levels began to rise again. This is similar to the course observed in humans as metastatic prostate cancer reaches the hormone-refractory stage. Our results demonstrated that androgen ablation decreases BMD and %BV/TV in NT. The C4-2–osseous model therefore mimics the human situation, in which an osteoporotic response to androgen suppression is seen not only in the tumor but in the whole skeleton[35]. Evidently the model can be used to study both the interactions of CaP cells with the bone and the effects of androgen suppression on CaP bone metastasis. In summary, we shown that the C4-2–osseous model exhibits many aspects of bone metastases of advanced prostate cancer in patients, although it does not possess the overall osteoblastic character (increase in bone volume) which is the hallmark of CaP bone metastases in patients with advanced disease. However, bone resorption is believed to be an essential component in the establishment of bone metastases. Therefore, models demonstrating both bone resorption and formation can provide useful information related to perturbation of normal bone remodeling by CaP bone metastases.

After characterization of the C4-2 bone metastasis model we examined the effects of administration of ZA on C4-2 cell *in vitro* and *in vivo* (manuscript in preparation). C4-2 cells proliferation was inhibited by ZA and cells appearance was consistent with apoptosis (Figure 1).

Figure 1. Effects of ZA on C4-2 Prostate Cancer Cells *in Vitro.* C4-2 cells were treated with ZA for 4 days. Changes in proliferation were determined using Quick proliferation kit. Results were normalized to absorbance of untreated cells A. Effects on proliferation; B. Effects on morphology .* $p < 0.0001$

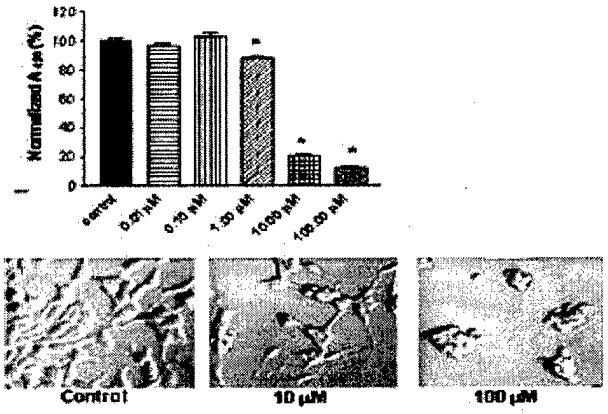

Both prevention and treatment regimens of administration of ZA abolished the decrease in BMD caused by C4-2 cells, and also led to significant increases in BMD in non-tumored tibiae. BHM analysis confirmed the expected effects of ZA on bone remodeling, showing increases in bone volume in tissue volume (BV/TV), and decreases in osteoblast and osteoclast surfaces per bone surface (Ob.S./BS and Oc.S./BS), under both regimens of administration. BHM analysis also showed decreased tumor volume (TuV/TV) after ZA administration. The results of bone histomorphometry (BHM) analysis are presented in Table 4, and representative examples of the histological appearance of tibiae with C4-2 cells with and without ZA administration are shown in Figure 5 , respectively. In contrast to the BHM results, which showed a decrease in TuV/TV, serum PSA levels were not significantly changed in animals receiving injections of ZA (Figures 6). We hypothesize that the discrepancy between serum PSA levels and decreased tumor volume as determined by BHM analysis is due to the different method used. Similar observations were presented at the ASBMR Annual Meeting—a discrepancy between BMH analysis results and total volume of metastases as determined by optical imaging. ##**Whose hypothesis? The plausible explanation is** The hypothesis hold that tumor growth is decreased next to the growth plate where the effects of ZA on bone are the most pronounced, but continues in lower parts of the tibiae. In summary with the DOD funding we have shown that ZA

Table 4. Results of Bone Histomorphometry Analysis of C4-2 Tibiae with and without Administration of ZA.

	Normal Tibiae	C4-2	ZA	
			C4-2 Treatment	C4-2 Prevention
Tumor volume (TuV/TV%)	na	55.33 ± 2.63	55.08 ± 4.38	11.86 ± 2.60
Trabeculae bone volume (BV/TV; %)	8.71 ± 0.91	4.82 ± 1.66	11.72 ± 1.94	52.56 ± 2.90
Trabeculae number (Tb.N.; #/mm^2)	2.79 ± 0.32	1.40 ± 0.42	2.95 ± 0.35	6.29 ± 0.39
Trabecular Thickness (Tb.Th.; mM)	31.09 ± 1.36	30.73 ± 2.62	39.28 ± 4.21	85.31 ± 7.93
Trabecular separation (mM)	362.7 ± 52.4	1373.0 ± 482.0	318.0 ± 40.6	76.1 ± 4.9
Osteoblast Surface (Ob.S./BS; %)	0.589 ± 0.194	6.820 ± 1.539	0.00	0.00
Osteoclast surface (Oc.S./BS; %)	5.48± 0.528	6.82 ± 1.54	0.460 ± 0.130	0.432 ± 0.109

can inhibit bone lysis associated with CaP tumors, and that it also exhibits growth-inhibitory effects on CaP tumors which are tumor-type dependent.

Figure 5.
Histology of C4-2 and Contralateral Tibiae of Animals after Administration of ZA

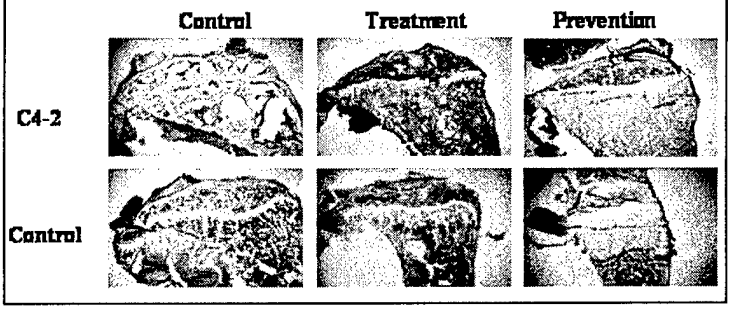

Figure 6. Serum PSA Levels in Animals with C4-2 Bone Metastasis with or without Administration of ZA.

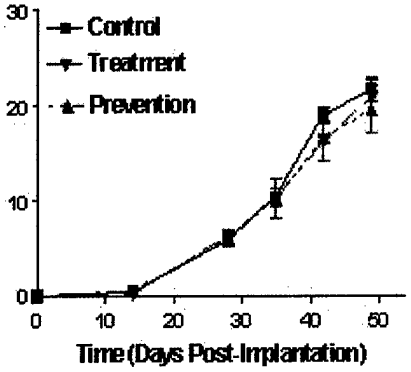

- **Determination of effects of BP on seeding of PC-3 following cardiac injection (months 24-36).**

In year 02 we transfected C4-2B cells with a plasmid containing enhanced green fluorescent protein (EGFP). Using clonal selection we have established a clone of C4-2B cells of which 95% are positive for expression of EGFP. Twenty SCID mice were injected with EGFP-C4-2B into the left cardiac ventricle. Half of the animals are being treated with ZA (100 mg/kg, twice a week). Animals are monitored for growth of CaP bone metastasis by measuring serum levels of PSA every two weeks. As of now no or extremely low PSA levels were detected in animals from both groups. The experiments have been underway for 3.5 months. We will follow the animals for a maximum of 5 months. Analysis of the presence of metastasis will be performed using fluorescent imaging by Anticancer, Inc.

KEY RESEARCH ACCOMPLISHMENTS for YEAR 03

- We have characterized the C4-2 model of prostate cancer metastasis and effects of ZA on the metastasis.
- We have not succeeded in abolishign expression of CatK in CaP cells.
- We have begun to evaluate whether ZA affects the spread and establishment of CaP metastasis.

REPORTABLE OUTCOMES

Publications:

Corey E, Brown LG, Quinn JE, Poot M, Roudier MP, Higano CS, and Vessella RL. Zoledronic acid exhibits anti-tumor effects on prostate cancer. *Clin Cancer Res* (attached).

Brubaker KD, Thomas R, Vessella RL, and **Corey E.** Expression and activity of Cathepsin K in prostate cancer. *J. Bone and Min. Res.* (attached).

Pfitzenmaier J, Quinn JE, Odman AM, Zhang J, Keller ET, Vessella RL, **Corey E.** Characterization of C4-2 Prostate Cancer Bone Metastases and Their Response to castration. Accepted for publication in *J. Bone and Min. Res.* (attached).

Abstracts:

Corey E. *et al.* Evaluation of Effects of Osteoprotegerin and Zoledronic Acid on C4-2 Prostate Cancer Bone Metastasis. Third North American Meeting on Skeletal Complication of Malignancies, Bethesda, MD, 2002.

Corey E. *et al.* Effects of zoledronic acid on prostate cancer. 23rd Annual Meeting of American Society for Bone and Mineral Research, Phoenix, AZ, 2001.

Brubaker KD, Thomas R, Vessella RL, and **Corey E.** Cathepsin K expression and activity in prostate cancer. 23rd Annual Meeting of American Society for Bone and Mineral Research, Phoenix, AZ, 2001.

CONCLUSIONS

During the three years of this award we have found the CatK message, protein and enzymatic activity in prostate cancer cells. We have also shown that CaP cells can degrade collagen and that levels of collagen degradation by CatK are increased in prostate cancer patients with bone metastases. However, since we have not succeeded in abolishing expression of CatK in CaP cells, we were not able to demonstrate the roles of CatK in CaP metastasis *in vivo.*

We have also shown that ZA inhibits proliferation of prostate cancer cells and induced apoptosis in these cells *in vitro.* Our *in vivo* experiments with prostate cancer bone metastases models have shown that ZA significantly inhibited osteolysis associated with CaP cells in bone

and also growth of osteoblastic CaP tumors. These results suggest that ZA would be of benefit in treatment of advanced prostate cancer. However we have also shown that the effects of ZA are variable depending on the type of CaP tumor. C4-2 cells, which result in a mixed reaction, responded much less favorably than the osteoblastic metastasis.

REFERENCES

1 Brubaker, K. D., Vessella, R.L., True, L. D., Thomas, R., and Corey, E. Cathepsin K mRNA and protein expression in prostate cancer progression. *J Bone Miner Res* 2003; 18:222-230.

2 Corey, E., Brown, L. G., Quinn, J. E., Poot, M., Roudier M.P, Higano, C. S., and Vessella R.L. Zoledronic acid exhibits inhibitory effects on osteoblastic and osteolytic metastases of prostate cancer. *Clin Cancer Res* 2003; 9: 95-306.

3 Rubin MA et al. Rapid ("warm") autopsy study for procurement of metastatic prostate cancer. *Clin Cancer Res* 2000; 6:1038-1045.

4 Bubendorf L et al. Metastatic patterns of prostate cancer: an autopsy study of 1,589 patients. *Hum Pathol* 2000; 31:578-583.

5 Shimazaki J et al. Clinical course of bone metastasis from prostatic cancer following endocrine therapy: examination with bone x-ray. *Adv Exp Med Biol* 1992; 324:269-275.

6 Urwin GH et al. Generalised increase in bone resorption in carcinoma of the prostate. *Br J Urol* 1985; 57:721-723.

7 Clarke NW, McClure J, George NJR. Morphometric evidence for bone resorption and replacement in prostate cancer. *Br J Urol* 1991; 68:74-80.

8 Roland, S. Calcium studies in ten cases of osteoblastic prostatic metastasis. *J Urol* 1958; 79, 339-342.

9 Coleman RE et al. Preliminary results of the use of urinary excretion of pyridinium crosslinks for monitoring metastic bone disease. *Br J Cancer* 1992; 65:766-768.

10 Ikeda I, Miura T, Kondo I. Pyridinium cross-links as urinary markers of bone metastases in patients with prostate cancer. *Br J Cancer* 1996; 77:102-106.

11 Major P et al. Zoledronic acid is superior to pamidronate in the treatment of hypercalcemia of malignancy: a pooled analysis of two randomized, controlled clinical trials. *J Clin Oncol* 2001; 19:558-567.

12 Green JR. Chemical and biological prerequisites for novel bisphosphonate molecules: results of comparative preclinical studies. *Semin Oncol* 2001; 28:4-10.

13 Berenson JR et al. Zoledronic acid reduces skeletal-related events in patients with osteolytic metastases. *Cancer* 2001; 91:1191-1200.

14 Delaiss'e JM, Eeckhout Y, Vaes G. Inhibition of bone resorption in culture by inhibitors of thiol proteinases. *Biochem J* 1980; 192:365-368.

15 Delaiss'e JM, Ledent P, Vaes G. Collagenolytic cysteine proteinases of bone tissue. Cathepsin B, (pro)cathepsin L and a cathepsin L-like 70 kDa proteinase. *Biochem J* 1991; 279P167-74:167-174.

16 Everts V et al. Degradation of collagen in the bone-resorbing compartment underlying the osteoclast involves both cysteine-proteinases and matrix metalloproteinases. *J Cell Physiol* 1992; 150:221-231.

17 Hill PA et al. Inhibition of bone resorption by selective inactivators of cysteine proteinases. *J Cell Biochem* 1994; 56:118-130.

18 Debari K et al. An ultrastructural evaluation of the effects of cysteine- proteinase inhibitors on osteoclastic resorptive functions. *Calcif Tissue Int* 1995; 56:566-570.

19 Kafienah W et al. Human cathepsin K cleaves native type I and II collagens at the N-terminal end of the triple helix. *Biochem J* 1998; 331:727-732.

20 Rieman DJ et al. Biosynthesis and processing of Cathepsin K in cultured human osteoclasts. *J Bone Miner Res* 1998; 23:S429.

21 Velasco G et al. Human cathepsin O. Molecular cloning from a breast carcinoma, production of the active enzyme in Escherichia coli, and expression analysis in human tissues. *J Biol Chem* 1994; 269:27136-27142.

22 Bromme D, Okamoto K. Human cathepsin O2, a novel cysteine protease highly expressed in osteoclastomas and ovary molecular cloning, sequencing and tissue distribution. *Biol Chem Hoppe Seyler* 1995; 376:379-384.

23 Littlewood Evans AJ et al. The osteoclast-associated protease cathepsin K is expressed in human breast carcinoma. *Cancer Res* 1997; 57:5386-5390.

24 Garrett IR. Bone destruction in cancer. *Semin Oncol* 1993; 20:4-9.

25 Galasko CSB. Mechanisms in bone destruction in the development of skeletal metastasis. *Nature* 1976; 263:507-508.

26 Galasko CSB, Bennet A. Relationship of bone destruction in skeletal metastases to osteoclast activation and prostaglandins. *Nature* 1976; 263:508-510.

27 Morgan HM, Meikle MC, Hill PA. Effect of breast tumor cells on bone resorption in vitro. *J Bone Miner Res* 1998; 23:s430.

28 Eilon G, Mundy GR. Direct resorption of bone by human breast cancer cells in vitro. *Nature* 1976; 263:726-728.

29 Clements JD et al. 8 Evidence that serum NTx (collagen-type I N-telopeptides) can act as an immunochemical marker of bone resorption. *Clin Chem* 1997; 43:2058-2063.

30 Apone S, Lee MY, Eyre DR. Osteoclast generate cross-linked collagen N-telopeptides (NTx) but not free pyrilidones when cultures on human bone. *Bone* 1997; 21:129-136.

31 Vandesompele J et al. Accurate normalization of real-time quantitative RT-PCR data by geometric averaging of multiple internal control genes. *Genome Biol* 2002; 3:RESEARCH0034.

32 Corey E et al. Zoledronic acid exhibits inhibitory effects on osteoblastic and osteolytic metastases of prostate cancer. *Clin Cancer Res* 9, 2003; 9:295-306.

33 Corey E et al. Establishment and characterization of osseous prostate cancer models: intra-tibial injection of human prostate cancer cells. *Prostate* 2002; 52; 20--33.

34 Zhang J et al. Osteoprotegerin inhibits prostate cancer-induced osteoclastogenesis and prevents prostate tumor growth in the bone. *J Clin Invest* 2001; 107:1235-1244.

35 Oefelein MG et al. Skeletal fracture associated with androgen suppression induced osteoporosis: the clinical incidence and risk factors for patients with prostate cancer. *J Urol* 2001; 166:1724-1728.

Zoledronic Acid Exhibits Inhibitory Effects on Osteoblastic and Osteolytic Metastases of Prostate Cancer[1]

Eva Corey,[2] Lisha G. Brown, Janna E. Quinn, Martin Poot, Martine P. Roudier, Celestia S. Higano, and Robert L. Vessella

Departments of Urology [E. C., L. G. B., J. E. Q., M. P. R., C. S. H., R. L. V.] and Pathology [M. P.], University of Washington, Seattle, Washington 98195

ABSTRACT

Purpose: **In this study we have examined the effects of zoledronic acid (ZA), a new-generation bisphosphonate, on prostate cancer (CaP) cells *in vitro*, and on both osteoblastic and osteolytic CaP metastases in animal models.**

Experimental Design: ***In vitro*****, CaP cells were treated with ZA, and the effects on proliferation, cell cycle, and apoptosis were determined.** ***In vivo*****, PC-3, and LuCaP 23.1 s.c. and tibial tumors were treated with ZA. Effects on bone and tumor were determined by histomorphometry and immunohistochemistry.**

Results: **ZA decreased proliferation of CaP cells, and caused G_1 arrest and apoptosis of CaP cells *in vitro*. *In vivo*, s.c. CaP tumor growth was not affected by ZA. However, growth of osteoblastic and osteolytic metastases of CaP was inhibited significantly *in vivo*. Matrix metalloproteinase-2, matrix metalloproteinase-9, and Cathepsin K levels were decreased in osteolytic bone metastases after ZA administration.**

Conclusions: **In conclusion, we have shown that ZA has significant antitumor effects on CaP cells *in vitro* and *in vivo*. Antiosteolytic activity and the antitumor effects of this compound could benefit CaP patients with bone metastases.**

INTRODUCTION

Bone is a very common site of CaP[3] metastases (1, 2), and bone metastases are responsible for most of the morbidity associated with this disease. In contrast to bone metastases of breast cancer and myeloma, which are mainly osteolytic, a high percentage of CaP metastases exhibit the radiographic appearance of osteoblastic lesions (3). Histomorphometric studies of CaP bone metastases have shown that some of the sclerotic lesions are actually mixed in nature, with increased activities of both osteoblasts and osteoclasts (4, 5). Roland (6) has introduced the hypothesis that every primary or metastatic cancer in bone begins with osteolysis. A number of studies have shown that patients with advanced CaP exhibit elevated levels of osteolytic bone resorption markers in urine and blood (7, 8). The preponderance of evidence indicates that osteolysis is present in CaP bone metastasis even when the overall character appears to be osteoblastic. It follows that the use of compounds inhibiting osteolysis could be beneficial to patients with advanced CaP.

BPs are nonhydrolyzable pyrophosphate analogs. BPs have been shown to have inhibitory effects on osteoclast generation, maturation, and activity, thereby reducing osteoclastic bone resorption (9–11). BPs are used to treat Paget's disease, hypercalcemia associated with cancer, and lytic metastases of breast cancer and myeloma. Metabolic bone disease of CaP and the rationale for the use of BPs in CaP were reviewed recently (12).

ZA is a new-generation BP with a side chain containing an imidazole ring, and is one of the most potent BPs (13, 14). Berenson *et al.* (15) reported reduction of rates of skeletal events in metastatic patients by ZA. The value and potential of ZA in treatment of patients with cancer-related bone disease were also reviewed recently (16).

Over the past few years investigators have examined BPs for direct effects on cancer cells. Various studies support the hypothesis that there are such direct effects of BPs (17–21). Animal studies have demonstrated that pretreatment of mice with risedronate and ibandronate before breast cancer cell inoculation caused a significant reduction in tumor burden in bone (22, 23). Peyruchaud *et al.* (24) reported inhibitory effects of ZA on osteolytic lesions of breast cancer *in vivo*, and Mundy *et al.* (25) reviewed preclinical studies with BPs, finding that they reduced skeletal metastases, and that skeletal lesions and tumor burden were diminished by ZA. However, despite the extent of this work, the effects of ZA on CaP cells and CaP bone metastasis have not yet been studied in detail, although Lee *et al.* (26) have reported inhibition of CaP cell growth *in vitro* by ZA.

The mechanisms underlying BP effects on cancer cells are not well understood, and mechanistic studies have begun only recently. These mechanisms may involve apoptosis via interference with the mevalonate pathway (27–29) and activation of caspases (28), and/or effects on invasiveness of the target cells, mediated by changes in expression and activity of metallopro-

Received 5/31/02; revised 8/8/02; accepted 8/13/02.

The costs of publication of this article were defrayed in part by the payment of page charges. This article must therefore be hereby marked *advertisement* in accordance with 18 U.S.C. Section 1734 solely to indicate this fact.

[1] Supported by a University of Washington Royalty Research Award and United States Army Medical Research Material Command Prostate Cancer Research Program DAMD17-00-1-0529.

[2] To whom requests for reprints should be addressed, at Department of Urology, Mailstop 356510, University of Washington, Seattle, WA 98195. Phone: (206) 543-1461; Fax: (206) 543-1146; E-mail: ecorey@u.washington.edu.

[3] The abbreviations used are: CaP, prostate cancer; BP, bisphosphonate; ZA, zoledronic acid; MMP, matrix metalloproteinase; DAPI, 4′,6-diamidino-2-phenylindole; TUNEL, terminal deoxynucleotidyl transferase (Tdt)-mediated nick end labeling; TuV, tumor volume; TV, tissue volume; BV, bone volume; Tb.N., trabecular number; Tb.Sp., trabecular separation; Tb.Th., trabecular thickness; Ob.S., osteoblast surface; BS, bone surface; Oc.S., osteoclast surface; FBS, fetal bovine serum.

teinases. Tumor cell invasion and metastasis are at least partially mediated by MMPs, through their ability to digest basement membrane and extracellular matrix components. Two published studies have demonstrated convincingly that secretion of MMP-1 and MMP-2 is affected by BP (20, 30), whereas a study by Farina *et al.* (31) showed that BP affected the activation of MMP-2. The association of MMP-2 with PC-3 invasiveness and metastatic character also suggests a role for this proteinase in CaP metastasis.

We have examined the effects of ZA on CaP cells *in vitro* and *in vivo*. Our results show that ZA directly inhibits CaP proliferation and enhances apoptosis of CaP cells *in vitro*, and also reduces growth of CaP tumors in murine bone. These findings, combined with reports of increased osteolysis in CaP patients, indicate potential benefits of using ZA in treating CaP metastases, possibly involving a combination of effects on bone resorption and direct effects on tumor cells.

MATERIALS AND METHODS

CaP Cell Lines and Xenografts. LNCaP and PC-CaP cell lines, and CEM, an acute lymphoblastic leukemia cell line (American Type Culture Collection, Rockville, MD), were maintained under standard culture conditions. LuCaP 23.1, a PSA-producing human CaP xenograft (32), is passaged s.c. in male athymic mice (BALB/c *nu/nu*; Simonsen Laboratories, Gilroy, CA).

Cell Proliferation. LNCaP and PC-3 cells were allowed to adhere overnight in 96-well plates. RPMI 1640 without phenol red with 10% or 2% FBS was used for the experiments. ZA was dissolved in 100 mM PBS (pH 7.2) and added to the medium. Cells were treated with 4.1 nM to 340 μM ZA for 1, 2, 3, or 4 days. The Quick Cell Proliferation Assay kit (BioVision Laboratories, Mountain View, CA) was used to measure the effects of ZA on cell proliferation. Experiments were repeated three times and done in triplicate; Student's *t* test was used to determine statistical significance.

Effects of ZA on Apoptosis and Cell Cycle Distribution. LNCaP and PC-3 cells were grown in RPMI 1640 without phenol red with 10% FBS and 68 μM ZA for 1, 2, or 3 days. Control cultures did not contain ZA. Semiconfluent attached and floating cells were harvested, counted, and resuspended to yield 10^6 cells in 1 ml of PBS. CEM cells were incubated with 0.3 μM camptothecin (Sigma, St. Louis, MO) for 3 h and used as a positive control for apoptosis.

TUNEL Assay. The TUNEL assay was used to determine effects of ZA on DNA fragmentation (33). One × 10^6 cells were fixed in 2% paraformaldehyde and refrigerated for 15 min. Cells were spun down and washed with PBS. Ice-cold ethanol was added drop-wise (3 volumes of cells), and the samples were stored at −20°C until the analysis. Untreated cells stained with DAPI (5 μg/ml; Accurate Chemical & Scientific Corporation, Westbury, NY) were used for each cell type as a control for autofluorescence. Treated and untreated cells (0.5 × 10^6) were mixed with 50 μl of TdT reaction mixture with or without 10 units of TdT enzyme (Boehringer Mannheim, Indianapolis, IN) and incubated for 1.5 h at 37°C. After washing with 1 ml of 15 mM EDTA and 0.1% NP40, cells were resuspended in 200 μl of DAPI. For each sample, 40,000 particles were analyzed (Coulter Epics Elite cytometer; Beckman Coulter, Fullerton, CA) using 10 mW UV excitation at 360 nm and 15 mW excitation at 488 nm. UV-excited DAPI fluorescence was collected with a 450/35 nm filter, whereas 488 nm-excited FITC fluorescence was collected with a 525/40 filter. All of the data were analyzed using custom software available commercially (Phoenix Flow3 Systems, San Diego, CA). Exact Fisher tests were used to determine statistical significance of the differences.

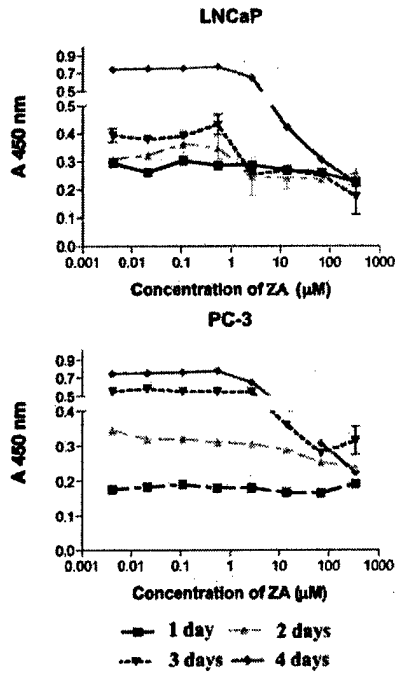

Fig. 1 Effects of ZA on proliferation of CaP cells. Proliferation of LNCaP and PC-3 cells was determined after exposure to ZA (0–340 μM) for 1, 2, 3, and 4 days with 10% FBS, using the Quick Proliferation kit as described in "Materials and Methods." Changes in absorbance at 450 nm were measured. Results are plotted as mean of A_{450} to demonstrate increased cell numbers as the experiments progressed; *bars*, ±SE. ZA (13.6 μM) was effective in inhibiting proliferation of all three CaP cell lines after 2 or more days of exposure.

CMXRosamine/MitoTracker Green FM Assay. Determinations of numbers of cells with compromised mitochondrial potential and cell cycle analysis were performed using MitoTracker Green FM, CMXRosamine, and Hoechst 33342 dyes, as described by Poot and Pierce (34). One μl of 200 μM CMXRosamine in DMSO, 1 μl of 200 μM of MitoTracker Green in DMSO, and 20 μl of 1 mM Hoechst 33342 in water were added to 1 × × 10^6 cells in 1 ml of medium, and the mixture was incubated at 37°C for 30 min in the dark. After incubation, cells were kept on ice until the flow cytometric analysis. Cells with lowered mitochondrial membrane potential (reduced red:green fluorescence ratio) were quantified by flow cytometry as described above. Hoechst staining was used to examine cell-cycle distribution. Only cells with unchanged mitochondrial potential were used to assess changes in cell-cycle distribution.

Animal Studies. For *in vivo* experiments we used PC-3 cells, yielding osteolytic bone lesions, and the xenograft LuCaP 23.1, which gives rise to osteoblastic lesions. All of the proce-

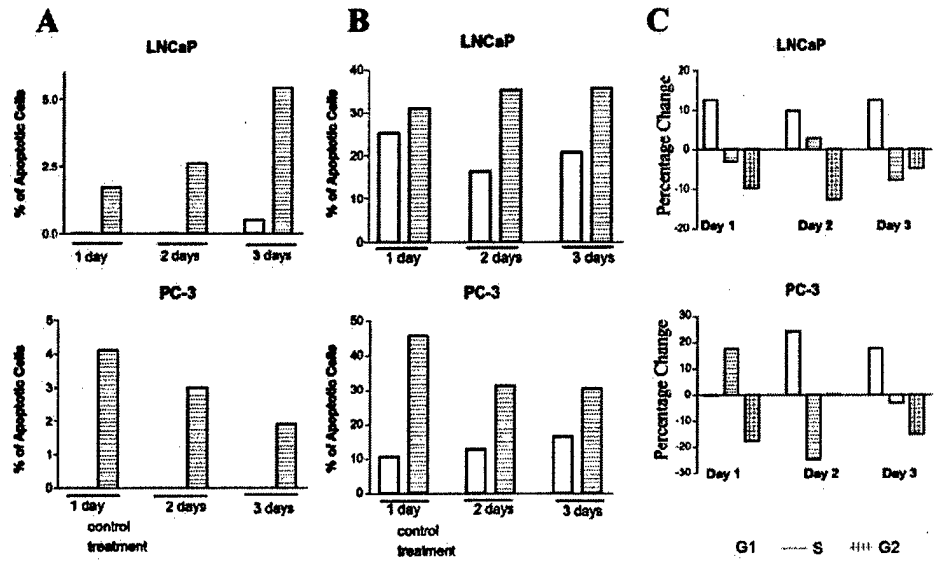

Fig. 2 Effects of ZA on apoptosis and cell-cycle distribution of CaP cells. LNCaP and PC-3 cells were treated with 68 μM ZA for 1, 2, and 3 days. Cells were processed for determination of apoptosis as described in "Materials and Methods." *A*, percentage of apoptotic cells after treatment with 68 μM ZA as determined by the TUNEL assay. A representative sample of results is shown. ZA treatment caused a significant increase in apoptosis of LNCaP, which rose with the duration of exposure. ZA also caused a significant increase in apoptosis of PC-3 cells, but the largest percentage of apoptotic cells was detected after 1 day of treatment. *B*, percentage increase in compromised cells (cells with diminished mitochondrial potential) after treatment with 68 μM ZA. *C*, Hoechst staining was used to perform cell-cycle analysis of the portion of LNCaP and PC-3 cells with unchanged mitochondrial potential after treatment with 68 μM ZA for 1, 2, and 3 days. A representative example of the results is shown. ZA treatment caused G_1 arrest in LNCaP cells after 1, 2, and 3 days of exposure, and also in PC-3 cells after 2 and 3 days of exposure. One day of treatment of PC-3 cells caused a significant increase in the cell population in S phase.

dures were performed in compliance with the University of Washington Institutional Animal Care and Use Committee and NIH guidelines. Six-to-8-week-old male mice (Fox Chase SCID mice; Charles River, Wilmington, MA) were used for the s.c. injections, and 4–6-week-old male mice were used for tibial injections.

Effects of ZA on s.c. Tumors. Animals (10 in treatment groups and 5 in control groups) were injected s.c. with 2×10^6 PC-3 cells or implanted with LuCaP 23.1 tumor bits. After tumors reached ~200 mg, 5 μg of ZA was injected twice weekly s.c. TuV was measured twice weekly and calculated as $L \times H \times W \times 0.5236$. Animals were sacrificed when tumors reached ~1000 mg or when animals were becoming compromised.

Effects of ZA on Intratibial Tumors. Single-cell suspensions (2×10^5 cells in ~10 μl, PC-3 and LuCaP 23.1) were injected directly into the tibiae of intact male mice (SCID; Ref. 35). Two regimens of ZA administration were used: (*a*) for prevention, administration of ZA was started simultaneously with injection of tumor cell; this regimen was chosen to simulate potential effects of ZA on cells arriving at the metastatic site, thereby revealing potential interference with establishment of metastases; and (*b*) for treatment, administration of ZA was started when the tumor was established, simulating treatment of established metastatic disease (LuCaP 23.1: PSA level ~5–10 ng/ml, 33 days after injection of tumor cells; PC-3: 7 days after injection of tumor cells). Under each regimen, 5 μg of ZA was injected twice weekly s.c.. Blood was drawn every 2 weeks for determination of PSA serum levels (LuCaP 23.1 only). Before sacrifice, the animals were anesthetized, and a flat plate radiograph was taken with a diagnostic mammography unit (35 kV, 2.3 s, 20.7 mA/s, small focal setting). Of the animals with PC-3 cells in tibiae, the control group and 5 animals from each ZA-administration group were sacrificed 4 weeks after injection of cells when the control animals were becoming compromised. The remaining animals bearing PC-3 cells in tibiae, which were all ZA-treated animals, were sacrificed at a later time, when the animals were becoming compromised (7–9 weeks after injection). Animals bearing LuCaP 23.1 were sacrificed based on radiographic appearance of the tibiae indicating extensive osteoblastic reaction. Tumor growth of LuCaP 23.1 in tibia depends significantly on the single-cell preparation; therefore we implanted 5 animals of the control group with the same preparation as animals of the prevention group, and, separately, 5 animals of the control group with the same preparation as animals of the treatment group. Animals of the prevention group and the corresponding control animals were sacrificed 130 days after injection of LuCaP 23.1 cells. ZA-treated animals under the treatment regimen and corresponding control animals were sacrificed 90 days after injection of the LuCaP 23.1 cells. After sacrifice the tumor-bearing tibiae were harvested. Samples were divided for histomorphometric analysis (embedding in methacrylate; Ref. 36) or for histology and immunohistochemistry [fixed in 10% neutral NBF for 24 h, decalcified in 10% formic acid as described (37), and embedded in paraffin]. The contralateral tibiae of animals were harvested, embedded in methacrylate, and used as controls for histomorphometric analysis.

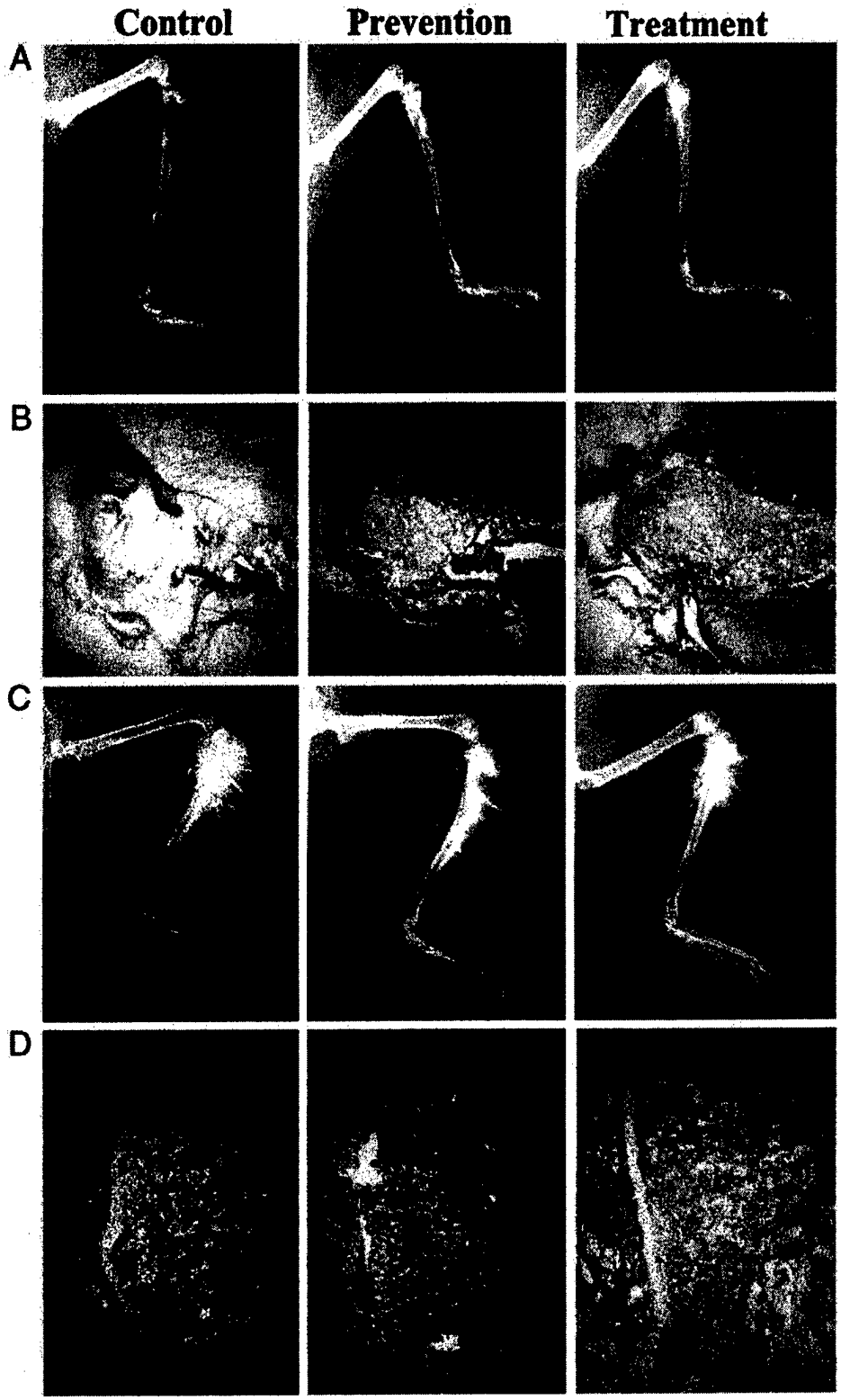

Fig. 3 Radiography and histology of PC-3 and LuCaP 23.1 in tibiae after ZA treatment. *A*, representative radiographs of PC-3 tumors in tibiae. Tibiae of SCID mice were injected with PC-3 cells, and ZA was administered under prevention and treatment regimens as described in "Materials and Methods." Animals were sacrificed 4 weeks after injection and radiographs were taken using a mammography unit. PC-3 cells cause a strong osteolytic reaction in the bone, with destruction of a large portion of mineralized tissue (*control*). ZA administration (*prevention* and *treatment*) decreased the bone lysis caused by PC-3 cells; radiographs show conservation of tibiae with increased density of bone. *B*, representative histology

Histomorphometric Analysis. Analysis was performed on 5-μm sections of methacrylate-embedded tibiae stained with Goldner's stain as described (38). Histomorphometric determinations of TuV of PC-3 tumors and BV were performed on a TV of 0.604 mm^2 adjacent to the growth plate using an Osteomeasure Image Analysis system (Osteometrics, Atlanta, GA). Percentages of BV and TuV in TV were calculated. Analysis of LuCaP 23.1 was performed by Skeletech, Inc. (Bothell, WA). Analysis was performed on mouse proximal tibiae. BV, TuV, Tb.N. (number/mm), Tb.Sp. (μm), Tb.Th. (μm), Ob.S/BS (%), and Oc.S/BS (%) were determined. Statistical analysis was performed using Student's *t* test.

Immunohistochemical Analysis. Staining was performed to determine expression of Cathepsin K (anti-Cathepsin K chicken polyclonal antibody, 1:25 dilution; Immunodiagnostics System Ltd., Boldon, United Kingdom), MMP-2 (anti-MMP-2 rabbit polyclonal antibody, 5 μg/ml; Chemicon International Inc., Temecula, CA), and MMP-9 (anti-MMP-9 rabbit polyclonal antibody, 5 μg/ml; Chemicon International). Immunoperoxidase staining was performed as we described previously (39), with modifications to the serum blocking process. The serum block contained rabbit, horse, and goat serum (5% each) for the anti-Cathepsin K antibody, and horse, goat, and chicken serum (5% each) for the anti-MMP-2 and anti-MMP-9 antibodies, to prevent nonspecific binding in the xenograft tissues. Antigen retrieval was performed in 10 mM citrate buffer (pH 6) for 10 min before staining with the anti-MMP-2 and MMP-9 antibodies. The primary antibodies were diluted in the serum blocking solution, as were the appropriate negative controls (chicken IgY and rabbit IgG, respectively). Detection of immunoreactivity was performed using avidin-biotin complex method kits (Vector Laboratories, Burlingame, CA) and 3,3′-diaminobenzidine as substrate.

RESULTS

Effects of ZA on Proliferation of CaP Cells. ZA (340 μM) inhibited proliferation of LNCaP and PC-3 cells in the presence of 10% FBS by up to 70% after 4 days of treatment (Fig. 1). Treatment with 13.6 μM ZA caused significant inhibition (15–45%) of proliferation after 2 or more days of exposure in both cell lines tested ($P = 0.05–0.00001$); however, 1 day of treatment was not effective. Similar effects were observed with 2% FBS (data not shown).

Effects of ZA on Apoptosis and Cell Cycle of CaP Cells. To evaluate effects of ZA on apoptosis we used 68 μM ZA, which decreased proliferation of all three of the cell lines by ≥25% after 2 and 3 days of exposure. Using the TUNEL assay to detect DNA fragmentation, we observed 1.9, 2.2, and 2.6% apoptotic cells in the ZA-treated LNCaP cells after 1, 2, and 3 days of exposure, respectively, with no significant apoptosis detected in untreated cells (0.1, 0, and 0.5%; Fig. 2*A*). PC-3 cells treated with 68 μM of ZA showed an increase in apoptosis to 4.1% after 1 day of treatment, and 3% and 1.8%, respectively, after days 2 and 3 of treatment with no significant apoptosis detected in untreated cells (Fig. 2*A*). Differences were significant as determined by Fisher's exact test ($P < 0.001$).

To confirm the increase in apoptosis we used an independent method. Detection of cells with compromised mitochondrial membrane potential (cells considered to be committed to the apoptotic pathway) also demonstrated an increase in the percentage of apoptotic cells after treatment with 68 μM of ZA (Fig. 2*B*). LNCaP cells exhibited significant increases after 1, 2, and 3 days of treatment (31.1 *versus* 25.3%, 35.2 *versus* 16.3%, and 35.7 *versus* 20.8%, respectively). Similar results were obtained with PC-3 cells, with the greatest difference appearing on day 1 (45.7 *versus* 10.8%, 31.4 *versus* 12.9%, and 30.5 *versus* 16.7%). All of the differences were significant as determined by Fisher's exact test ($P < 0.0001$).

We also examined the cell-cycle distribution of CaP cells, using only the population of cells with unchanged mitochondrial potential. Treatment of LNCaP cells with 68 μM ZA for 1, 2, and 3 days increased the proportion of cells in G_1 phase by 9.8–12.6% over the control, indicating G_1 arrest (Fig. 2*C*), with concomitant decreases in cell populations in S and G_2 phases. Treatment of PC-3 cells with 68 μM of ZA caused a significant increase in percentages of cells in S phase after 1 day of treatment (17.5%), with a decrease in populations of cells in G_2 phase. This was followed by increases in G_1-phase cells after 2 and 3 days (24.3% and 17.7%, respectively), with concomitant decreases in S and G_2 phases (Fig. 2*C*).

Effects of ZA on CaP *in Vivo*. For *in vivo* experiments we used two CaP models: PC-3 cells, which are responsive to ZA *in vitro* and yield lytic bone metastases, and LuCaP 23.1, which does not grow *in vitro* but is one of the few CaP xenografts that gives rise to osteoblastic bone metastases (40). We first examined effects on s.c. tumors. In contrast to the *in vitro*

of PC-3 tumors in tibiae. Tibiae of SCID mice were injected with PC-3 cells, and ZA was administered under prevention and treatment regimens as described in "Materials and Methods." Tibiae were harvested and embedded in methacrylate. Goldner staining was performed on 4-μM sections as described in "Materials and Methods." Tumor cells are *white* and *gray* in this picture; mineralized bone is *green*. The control tibia shows destruction of most of the mineralized bone. In the tibiae from prevention and treatment groups, the bone cortical shaft appears to be conserved. *C*, representative radiographs of LuCaP 23.1 Tumors in tibiae. Tibiae of SCID mice were injected with LuCaP 23.1 cells, and ZA was administered under prevention and treatment regimens as described in "Materials and Methods." Radiographs were taken using a mammography unit. LuCaP 23.1 cells caused a strong osteoblastic reaction in the bone in all three groups (*control, prevention,* and *treatment*). *D*, representative histology of LuCaP 23.1 Tumors in tibiae. Tibiae of SCID mice were injected with PC-3 cells, and ZA was administered under prevention and treatment regimens as described in "Materials and Methods." Tibiae were harvested and embedded in methacrylate. Goldner staining was performed on 4-μM sections as described in "Materials and Methods." Tumor cells are *white* and *gray* in this picture; mineralized bone is *green*. The control example (untreated tibia with LuCaP 23.1) shows extension of mineralized bone beyond the former cortical shaft. Many trabeculae and tumor foci are observed. In tibiae of ZA-treated animals (*prevention* and *treatment*) mineralized bone also extends beyond the original cortical shaft, but is not as "spread out" as in untreated animals. In addition, the trabeculae are thicker *versus* the untreated LuCaP 23.1 tibiae, and their separation is smaller. Tumor foci appear smaller, suggesting effects of ZA on TuV.

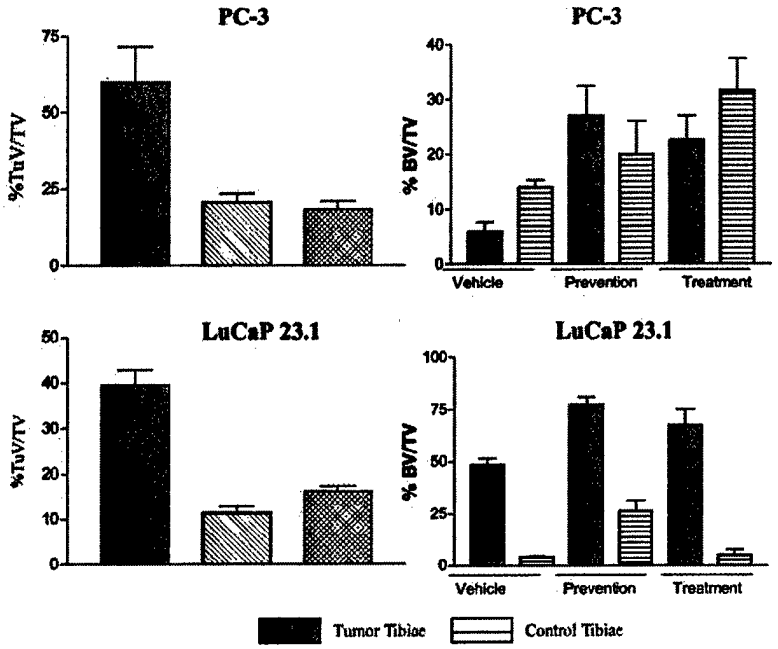

Fig. 4 Bone histomorphometric analysis of effects of ZA on PC-3 and LuCaP 23.1 in tibiae. Tibiae with PC-3 or LuCaP 23.1 with or without ZA administration were embedded in methacrylate and used for bone histomorphometrical analysis as described in "Materials and Methods." Analysis was performed on a tissue area adjacent to the growth plate. *A,* the percentage of TuV/TV was calculated based on the measurement of TuV in Goldner-stained sections of tibiae. Results are plotted as mean; *bars,* ±SE. Percentage TuV/TV was decreased in the animals after ZA administration, suggesting effects of ZA on CaP tumor cells. *B,* tibiae with and without tumors were harvested and embedded in methacrylate. Analysis of changes in BV was performed on Goldner-stained sections. The percentages of BV/TV in tibiae with tumors and contralateral tibiae were calculated. Results are plotted as mean; *bars,* ±SE. PC-3 cells cause lysis of bone, which is decreased by administration of ZA. LuCaP 23.1 cells cause bone formation, and this effect is augmented by administration of ZA.

results, we did not detect significant decreases in TuVs of s.c. PC-3 and LuCaP 23.1 xenografts treated with ZA *versus* untreated animals. However, when we examined the effects of ZA on both tumors and bones with PC-3 and LuCaP 23.1 grown in tibiae, we detected significant increases in BV and decreases in TuV under both regimens of administration (prevention and treatment). Representative examples of radiographs and histology are shown in Fig. 3, *A* and *B* (PC-3) and Fig. 3, *C* and *D* (LuCaP 23.1). The take rate of PC-3 in tibiae was 100% (10 of 10) in all three of the groups, and was unaffected by ZA administration. Percentage TuV/TV of PC-3 cells was significantly smaller in tibiae of ZA-treated animals *versus* control animals (Fig. 4*A,* control: 59.8 ± 11.6%, prevention: 20.7 ± 2.9%, $P = 0.029$, treatment: 18.3 ± 2.8%, $P = 0.022$). PC-3 cells caused the osteolytic reaction in bone, leading to a significant reduction in %BV/TV in comparison to contralateral tibiae (Fig. 4*B,* 5.9 ± 1.7%, *versus*13.9 ± 1.4%; $P = 0.0024$). Comparison of %BV/TV of tumored and contralateral tibiae after administration of ZA showed that %BV/TV of tumored tibiae was not significantly different from %BV/TV of contralateral tibiae of the same animals (Fig. 4*B,* prevention: 26.9 ± 5.5% *versus* 19.9 ± 6.1%, $P = 0.19$, and treatment: 22.5 ± 4.6% *versus* 31.6 ± 5.9%, $P = 0.26$). Thus the effects of ZA were not restricted to the tumor site. However, there were significant increases in %BV/TV in both tumored and contralateral tibiae accompanying the ZA administration compared with vehicle alone (Fig. 4*B;* $P < 0.01$). The animals in the control group became compromised at week 4 and were, therefore, sacrificed; however, the ZA-treated animals under both regimens with PC-3 cells in tibiae did not become compromised until weeks 7–9, at which time they were sacrificed.

Because many CaP bone metastases have the radiographic appearance of osteoblastic reactions, we performed a more detailed analysis of the LuCaP 23.1 bone metastases. Take rates of LuCaP 23.1 were similar in control and ZA-treated groups (100%; 10 of 10), suggesting that ZA administration did not affect establishment of the cells in the bone milieu. The percentage of TuV/TV of LuCaP 23.1 in tibiae was significantly smaller in ZA-treated animals *versus* untreated animals (Fig. 4*A,* prevention: $P = 0.001$, treatment: $P = 0.009$; Table 1). Our data also showed that PSA serum levels in animals bearing LuCaP 23.1 xenografts were significantly decreased by ZA under prevention and treatment regimens *versus* control animals (Fig. 5), suggesting decreased tumor growth, based on the assumption that PSA serum levels are correlated positively with TuV. These results are in agreement with our observation that ZA *in vitro* had inhibitory effects on tumor growth. LuCaP 23.1 xenografts cause an osteoblastic reaction in bone, leading to a significant increase in %BV/TV *versus* contralateral tibiae ($P = 0.0008$). Administration of ZA under both regimens to animals bearing LuCaP 23.1 tumors in tibiae additionally increased the %BV/TV of tumored tibiae *versus* contralateral tibiae (prevention: $P = 0.017$, treatment: $P = 0.017$; Fig. 4*B;* Table 1). Analysis of tibiae from control animals (two groups, sacrificed 130 and 69 days after tumor cell injection) showed no significant differences in the parameters evaluated (%BV/TV, %TuV/TV, Tb.N., Tb.Th., Tb.Sp., Ob.S./BS, and Oc.S./BS). Therefore, for histomorphometrical analysis of the effects of ZA administration, the control tibiae were treated as one group. There were no significant changes in Tb.N. with ZA administration, but we observed significant decreases in Tb.Sp. and increases in Tb.Th., which did not reach significance. Ob.S./BS was greater in tibiae bearing LuCaP 23.1 *versus* contralateral tibiae, but remained approximately the same in ZA-treated animals *versus* untreated animals. However, in keeping with the known antiosteoclastic activity of ZA, the Oc.S./BS was lower in ZA-treated

Table 1 Results of bone histomorphometrical analysis of LuCaP 23.1 in bone with and without ZA treatment
Analysis was performed on 2–5 samples. Results are presented as a mean ± SE. Significance of results was determined using Student's *t* test.

		LuCaP 23.1 control	LuCaP 23.1/ZA prevention	LuCaP 23.1/ZA treatment
% TuV/TV		39.6 ± 3.3	11.4 ± 1.5[a]	16.2 ± 1.0[b]
% BV/TV	Tumor tibiae	48.4 ± 3.1	76.9 ± 3.9[b]	67.2 ± 7.8[c]
	Contralateral tibiae	4.2 ± .4	26.2 ± 5.3[b]	5.0 ± 2.7
Tb.N.	Tumor tibiae	7.8 ± .3	8.2 ± 1.3	8.4 ± 0.5
	Contralateral tibiae	1.7 ± .04	6.8 ± 1.1[b]	1.7 ± 0.9
Tb.Th.	Tumor tibiae	62.9 ± 5.6	99.6 ± 19.0	79.8 ± 4.8
	Contralateral tibiae	34.5 ± 3.0	37.8 ± 2.2	29.6 ± 0.9
Tb.Sp.	Tumor tibiae	66.5 ± 4	28.0 ± 0.5[a]	39.7 ± 11.5[c]
	Contralateral tibiae	643.4 ± 121.4	118.3 ± 30.8[c]	782.8 ± 415.8
Ob.S./BS	Tumor tibiae	3.8 ± 0.6	3.1 ± 1.0	5.5 ± 5.4
	Contralateral tibiae	0.00	0.6 ± 0.3	2.7 ± 2.0
Oc.S/BS	Tumor tibiae	2.9 ± 1.4	0.6 ± 0.3	1.1 ± 0.9
	Contralateral tibiae	6.3 ± 2.1	3.6 ± 1.1	1.5 ± 1.5

[a] $P < 0.001$.
[b] $P < 0.01$.
[c] $P < 0.05$.

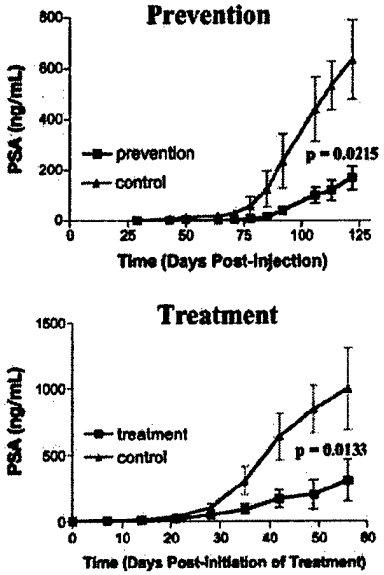

Fig. 5 Effects of ZA on PSA levels in animals with LuCaP 23.1 in tibia. Animals were injected with single-cell suspensions of LuCaP 23.1 in tibiae. ZA was administered SC twice weekly under two regimens. *1, prevention:* ZA injections started at the same time as cell injection. *2, treatment:* ZA injection started when PSA levels reached approximately 5–10 ng/ml, indicating established tumor in the bone. Blood was drawn for determination of PSA every 2 weeks. Results are plotted as mean; *bars,* ±SE. Significant differences in PSA serum levels were detected under both regimens of ZA administration in comparison with untreated LuCaP 23.1 tumors.

animals *versus* untreated animals and also in tibiae bearing LuCaP 23.1 *versus* contralateral tibiae, although these differences did not reach statistical significance.

Because ZA affects osteoclasts and their ability to degrade bone extracellular matrix, we examined levels of expression of Cathepsin K, a cysteine protease responsible for degradation of collagen in CaP cells. We detected immunoreactivity of Cathepsin K in PC-3 cells grown in tibiae, and this expression was decreased in PC-3 cells in tibiae from ZA-treated animals under both regimens (Fig. 6*A*; Table 2). Interestingly, Cathepsin K expression was not affected in LuCaP 23.1 xenografts in tibiae (Fig. 6*B*). Human bone with CaP metastasis used as a positive control exhibited strong staining in osteoclasts lining the BS. The same samples treated under the same conditions with chicken IgY were negative. A similar pattern was observed with MMP-2 and MMP-9. MMP-2 and MMP-9 expression was decreased in PC-3 cells in tibiae by ZA treatment (Fig. 7; Table 2), but no corresponding changes were observed in LuCaP 23.1 cells. The same samples stained with rabbit IgG exhibited no immunoreactivity.

DISCUSSION

Our data show that ZA has direct antiproliferative and apoptotic effects on CaP cells *in vitro*. The degree of inhibition of proliferation varied with the CaP cell line, but it is unclear whether this is connected with known phenotypic differences among these cell lines; mechanistic studies will be required to answer this question. Our data are in agreement with a recent report of Lee *et al.* (26), who also observed similar inhibitory effects of ZA on proliferation of CaP cells *in vitro*. The concentrations effective *in vitro* are higher than those used under clinical conditions, but because BPs accumulate in bone (41), the local concentrations might be considerably higher than those calculated on an organismal basis, conceivably reaching levels similar to those effective *in vitro*.

Several studies have suggested that BPs promote apoptosis of osteoclasts (11, 42). Apoptosis is characterized by various cellular changes, including DNA fragmentation, mitochondrial swelling, and chromatin condensation. We have used two independent assays to examine activation of apoptotic pathways. By detecting DNA fragmentation we observed an increase of up to 2.5-fold in apoptosis in LNCaP and PC-3 associated with ZA treatment, although the overall percentages of cells exhibiting DNA fragmentation were low. Assays of mitochondrial membrane potential as an indication of apoptosis also showed that ZA caused apoptosis of CaP cells. The time dependence of the results showed similar patterns: increased apoptosis was asso-

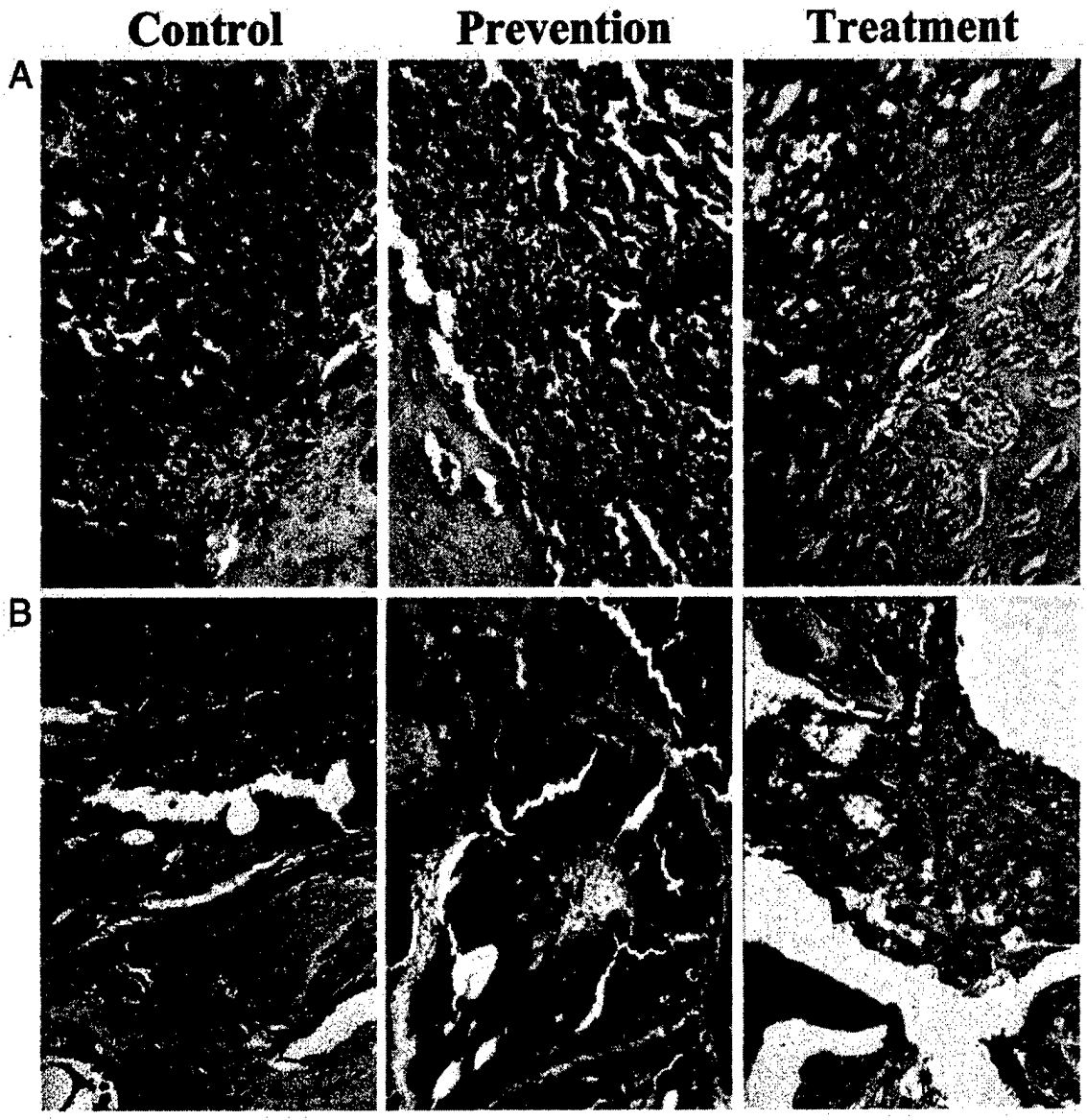

Fig. 6 Presence of Cathepsin K immunoreactivity in PC-3 and LuCaP 23.1 tumors in tibiae with and without ZA administration. Immunoreactivity of Cathepsin K, an enzyme involved in degradation of bone extracellular matrix, in representative samples of untreated and treated tibiae with PC-3 (*A*) and LuCaP 23.1 (*B*). Staining was performed as described in "Materials and Methods." Expression of Cathepsin K in PC-3 cells is decreased in tibiae after ZA administration under both prevention and treatment regimens *versus* control (untreated) tumored tibiae. In contrast Cathepsin K expression was not changed in osteoblastic, LuCaP 23.1 metastases.

ciated with longer exposure of LNCaP to ZA in each case, whereas the highest level of apoptosis of PC-3 was seen at 24 h. The difference between percentages of apoptotic cells as determined by TUNEL *versus* the mitochondrial assay is probably related to the kinetics of apoptosis. Mitochondria lose their function early in the apoptotic process, as reflected in a lowered mitochondrial membrane potential, whereas degradation of DNA and formation of apoptotic fragments are late events. Therefore, the time window during which a cell exhibits a lowered mitochondrial membrane potential is longer. Our data contrast with results published by Lee *et al.* (26), who reported that ZA did not cause apoptosis in CaP cells (DU 145 and PC-3). The differences between our results and those of Lee *et al.* (26) may be due to differences in the sensitivity of the methods used for determination of apoptosis, and/or to variations in the cultured cell lines.

There were significant differences in the responses of the LNCaP (hormone-sensitive) and PC-3 (hormone-insensitive) cell lines to ZA. The p53-deficient PC-3 (43) exhibited high levels of apoptosis and accumulation in S phase after 24 h, whereas LNCaP cells, with wild-type p53 (44), exhibited a slow rise in apoptotic cells, concomitant with a strong G_1 phase

Table 2 Immunohistochemical analysis of PC-3 and LuCaP 23.1 in tibiae after administration of ZA

	Control		Prevention		Treatment	
	Percentage of positive cells	Intensity of staining	Percentage of positive cells	Intensity of staining	Percentage of positive cells	Intensity of staining
PC-3						
Cathepsin K	20–40%	1+	0		0	
MMP-2	70–90%	2+	50%	1+	50–70%	1+
MMP-9	90%	2–3+	80–90%	1+	80%	1+
LuCaP 23.1						
Cathepsin K	80–90%	2+	80–90%	2+	80–90%	2+
MMP-2	80–90%	2–3+	80–90%	2–3+	80–90%	2–3+
MMP-9	80–90%	2–3+	80–90%	2–3+	80–90%	2–3+

arrest. We hypothesize that ZA induces apoptosis by distinct mechanisms, depending on the p53 status of the target cells. Cells that have lost their G_1/S checkpoint undergo rapid apoptosis (PC-3), whereas cells with functional p53 (as observed by arrest at the G_1/S border) still undergo ZA-induced apoptosis, albeit at a slower rate (LNCaP). A useful corollary is that the cytotoxic action of ZA on CaP cells does not appear to be dependent on p53 function.

To investigate *in vivo* the potential benefits of ZA to CaP patients we have examined the effects of ZA on s.c. CaP tumors and CaP bone metastases in animal models (40). The effects of ZA on s.c. tumors should be independent of the bone environment. In contrast with the *in vitro* inhibition data, we saw no significant effects of ZA on the growth of s.c. tumors. This may indicate that there are no direct effects of ZA *in vivo* under these conditions and that the observed effects on tumors in bone are all related to inhibition of osteolysis. An alternative hypothesis is that the lack of inhibitory effects on the s.c. tumors may be due to poor bioavailability of ZA, at least in part because the compound accumulates in bone. However, in osseous-CaP models, consisting of direct injection of CaP cells into tibiae, we observed inhibition of both tumor growth and bone degradation by ZA. It is not yet clear whether the two inhibitory phenomena are caused by a single or multiple activities of ZA. It has been suggested that factors released during degradation of bone extracellular matrix support growth of tumor cells (45). Zhang *et al.* (46) showed that administration of osteoprotegerin, a modulator of osteoclast recruitment and activity, can impede establishment of C4–2B metastases in bone when injected at the same time as the C4–2B cells, suggesting that osteoclastogenesis is an important mediator of establishment of CaP bone metastasis. The inhibition of tumor proliferation observed could be because of direct effects of ZA on tumor cells, indirect effects resulting from decreased bone lysis, a combination of these, or still other, unknown mechanisms. Our data indicate that ZA probably does not interfere with initial establishment of the tumors in bone, because the take rates were similar in control and prevention groups. Moreover, in the PC-3 intratibial tumors, ZA slowed but did not halt growth of the tumors, indicating that ZA may be palliative but not curative with osteolytic CaP metastases.

Results of BHM analysis also suggest that the increase in %BV/TV caused by LuCaP 23.1 may be partially due to *de novo* bone formation, because the Tb.N. in tumored tibiae is higher than in contralateral tibiae. However, the increase in BV/TV in ZA-treated animals bearing LuCaP 23.1 in tibiae *versus* nontreated animals appears to be due to increased thickness of trabeculae, which is consistent with decreased lysis and/or more bone formation in apposition to the existing trabeculae.

Cathepsin K, a cysteine protease expressed by osteoclasts, appears to be essential for osteoclast-mediated collagen type-I degradation (47). Cathepsin K is expressed in breast cancer cells (48), and we have reported recently on detection of Cathepsin K and its proteolytic activity in CaP tissues and CaP cell lines (49). In the studies presented here, ZA treatment decreased expression of Cathepsin K in PC-3 cells in bone. Reduced expression of Cathepsin K could also play a role in reduced degradation of bone by PC-3 tumors treated with ZA. However, the significance of unchanged levels of Cathepsin K in LuCaP 23.1 under ZA treatment needs to be determined. The difference between these two CaP xenografts suggests that more than one mechanism may be involved in the action of ZA and that the effective mechanisms may depend on the type of tumor.

To characterize additionally the direct effects of ZA on CaP xenografts *in vivo*, we examined expression of metalloproteinases MMP-2 and MMP-9, which are implicated in tumor cell migration, invasion, and bone extracellular matrix degradation in CaP tumors. Boissier *et al.* (20) showed that BPs affect invasiveness of breast and CaP cells. They associated this with inhibitory effects of BPs on the proteolytic activities of MMP-2, MMP-9, and MMP-12, but the actual production of MMP was unaffected. Teronen *et al.* (50) also reported decreased activity without decreased expression of MMP after BP treatment. We were unable to detect any proteolytic activity of MMP-2 and MMP-9 in the culture medium of CaP cells (data not shown), but we did observe reduced expression of MMPs 2 and 9 in osteolytic PC-3 tumors (but not in LuCaP 23.1 tumors) by immunohistochemistry. This represents a possible mechanism whereby ZA could directly inhibit the osteolytic activity of CaP tumors. In agreement with our results, Nemeth *et al.* (51) reported recently inhibition of PC-3 tumor-induced bone lysis by MMP inhibitors, additionally suggesting the importance of MMP in CaP lytic lesions.

In conclusion, we have shown that ZA has antiproliferative, apoptotic, and cytostatic effects on CaP cells *in vitro*. Significantly, ZA also has inhibitory effects on the growth of CaP osteoblastic and osteolytic bone metastases in an animal model, but we observed no inhibitory effects on CaP tumors outside of the bone milieu. The observation that ZA causes a

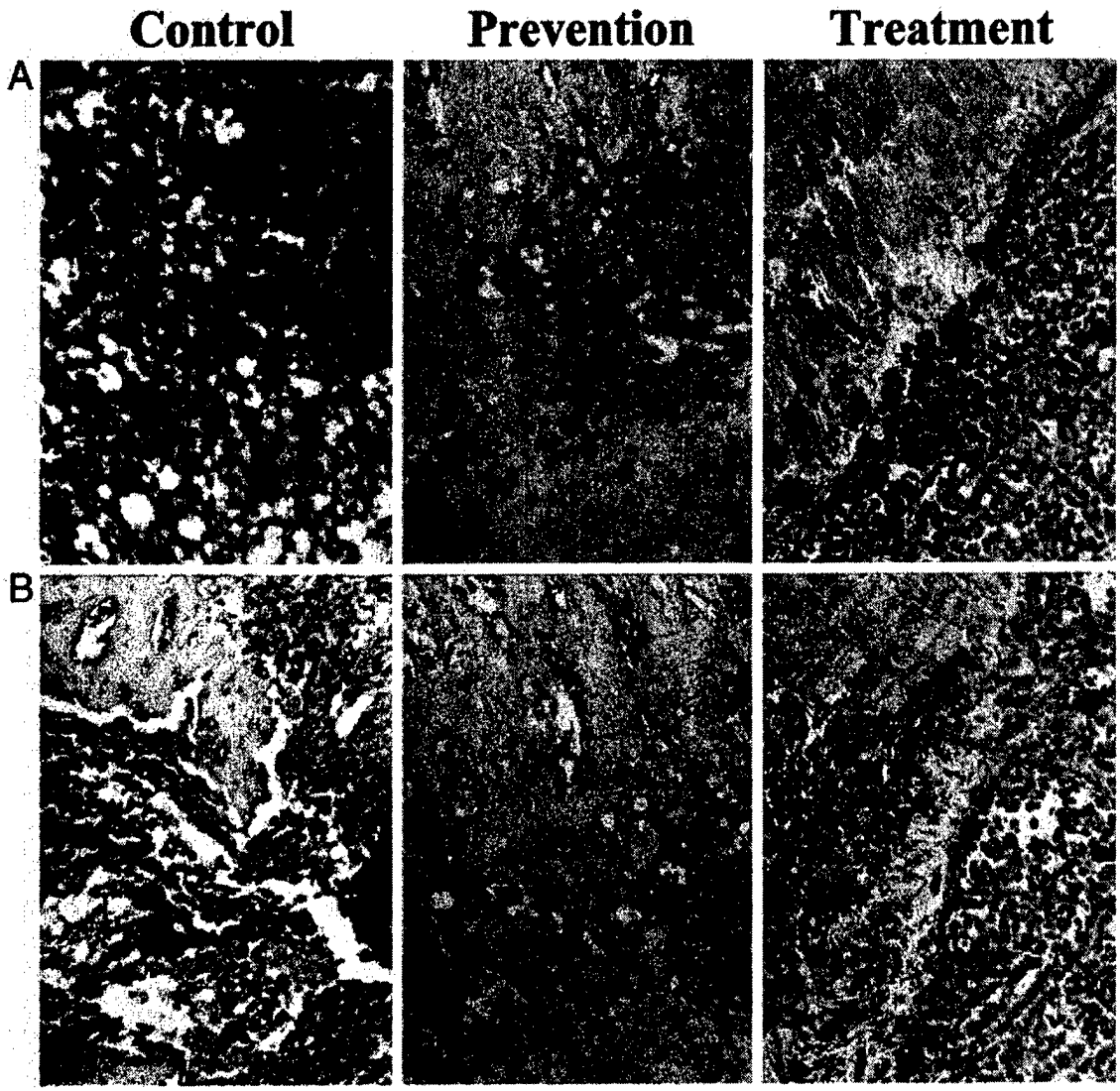

Fig. 7 Presence of MMP-2 and MMP-9 immunoreactivity in PC-3 in tibiae after administration of ZA. Effects of ZA on expression of MMP-2 and MMP-9 enzymes involved in degradation of bone extracellular matrix were examined by immunohistochemistry. Representative examples of MMP-2 (*A*) and MMP-9 (*B*) immunoreactivity in tibiae after ZA administration are shown. Both regimens of ZA administration appear to reduce immunoreactivity of MMP-2 and MMP-9 in osteolytic PC-3 metastases, suggesting possible mechanisms of direct effects of ZA on PC-3 cells resulting in decreased bone lysis.

reduction in expression of enzymes involved in bone degradation by PC-3 cells suggests a range of mechanisms by which ZA may inhibit CaP-induced bone lysis.

ACKNOWLEDGMENTS

Zoledronic acid was kindly provided by Pharma Novartis AG, Basel, Switzerland, and PSA assays by Abbott Laboratories, Abbott Park, IL. We thank Dr. Jonathan Green for helpful discussions and Dr. Michael Corey for useful comments and editorial help.

REFERENCES

1. Rubin, M. A., Putzi, M., Mucci, N., Smith, D. C., Wojno, K., Korenchuk, S., and Pienta, K. J. Rapid ("warm") autopsy study for procurement of metastatic prostate cancer. Clin. Cancer Res., *6*: 1038–1045, 2000.

2. Bubendorf, L., Schopfer, A., Wagner, U., Sauter, G., Moch, H., Willi, N., Gasser, T. C., and Mihatsch, M. J. Metastatic patterns of prostate cancer: an autopsy study of 1, 589 patients. Hum. Pathol., *31:* 578–583, 2000.

3. Shimazaki, J., Higa, T., Akimoto, S., Masai, M., and Isaka, S. Clinical course of bone metastasis from prostatic cancer following endocrine therapy: examination with bone x-ray. Adv. Exp. Med. Biol., *324:* 269–275, 1992.

4. Urwin, G. H., Percival, R. C., Harris, S., Beneton, M. N., Williams, J. L., and Kanis, J. A. Generalised increase in bone resorption in carcinoma of the prostate. Br. J. Urol., *57:* 721–723, 1985.

5. Clarke, N. W., McClure, J., and George, N. J. R. Morphometric evidence for bone resorption and replacement in prostate cancer. Br. J. Urol., *68:* 74–80, 1991.

6. Roland, S. Calcium studies in ten cases of ost4eoblasti prostatic metastasis. J. Urol., *79:* 339–342, 1958.

7. Coleman, R. E., Houston, S., James, I., Rodger, A., Rubens, R. D., Leonard, R. C. F., and Ford, J. Preliminary results of the use of urinary excretion of pyridinium crosslinks for monitoring metastic bone disease. Br. J. Cancer, *65:* 766–768, 1992.

8. Ikeda, I., Miura, T., and Kondo, I. Pyridinium cross-links as urinary markers of bone metastases in patients with prostate cancer. Br. J. Cancer, *77:* 102–106, 1996.

9. Flanagan, A. M., and Chambers, T. J. Inhibition of bone resorption by bisphosphonates: interactions between bisphosphonates, osteoclasts, and bone. Calcif. Tissue Int., *49:* 407–415, 1991.

10. Rodan, G. A. Mechanisms of action of bisphosphonates. Annu. Rev. Pharmacol. Toxicol., *38:* 375–388, 1998.

11. Rogers, M. J., Watts, D. J., and Russell, R. G. Overview of bisphosphonates. Cancer (Phila.), *80:* 1652–1660, 1997.

12. Berruti, A., Dogliotti, L., Tucci, M., Tarabuzzi, R., Fontana, D., and Angeli, A. Metabolic bone disease induced by prostate cancer: rationale for the use of bisphosphonates. J. Urol., *166:* 2023–2031, 2001.

13. Major, P., Lortholary, A., Hon, J., Abdi, E., Mills, G., Menssen, H. D., Yunus, F., Bell, R., Body, J., Quebe-Fehling, E., and Seaman, J. Zoledronic acid is superior to pamidronate in the treatment of hypercalcemia of malignancy: a pooled analysis of two randomized, controlled clinical trials. J. Clin. Oncol., *19:* 558–567, 2001.

14. Green, J. R. Chemical and biological prerequisites for novel bisphosphonate molecules: results of comparative preclinical studies. Semin. Oncol., *28:* 4–10, 2001.

15. Berenson, J. R., Rosen, L. S., Howell, A., Porter, L., Coleman, R. E., Morley, W., Dreicer, R., Kuross, S. A., Lipton, A., and Seaman, J. J. Zoledronic acid reduces skeletal-related events in patients with osteolytic metastases. Cancer (Phila.), *91:* 1191–1200, 2001.

16. Fleisch, H. Zoledronic acid: an evolving role in the treatment of cancer patients with bone disease. Semin. Oncol., *28:* 45–47, 2001.

17. Diel, I. J., Solomayer, E. F., Costa, S. D., Gollan, C., Goerner, R., Wallwiener, D., Kaufmann, M., and Bastert, G. Reduction in new metastases in breast cancer with adjuvant clodronate treatment. N. Engl. J. Med., *339:* 357–363, 1998.

18. van der Pluijm, G., Vloedgraven, H., van Beek, E., van der Wee Pals, L., Lowik, C., and Papapoulos, S. Bisphosphonates inhibit the adhesion of breast cancer cells to bone matrices *in vitro*. J. Clin. Investig., *98:* 698–705, 1996.

19. Boissier, S., Magnetto, S., Frappart, L., Cuzin, B., Ebetino, F. H., Delmas, P. D., and Clezardin, P. Bisphosphonates inhibit prostate and breast carcinoma cell adhesion to unmineralized and mineralized bone extracellular matrices. Cancer Res., *57:* 3890–3894, 1997.

20. Boissier, S., Ferreras, M., Peyruchaud, O., Magnetto, S., Ebetino, F. H., Colombel, M., Delmas, P., Delaisse, J. M., and Clezardin, P. Bisphosphonates inhibit breast and prostate carcinoma cell invasion, an early event in the formation of bone metastases. Cancer Res., *60:* 2949–2954, 2000.

21. Stearns, M. E. Alendronate blocks TGF-β1 stimulated collagen 1 degradation by human prostate PC-3 ML cells. Clin. Exp. Metastasis, *16:* 332–339, 1998.

22. Sasaki, A., Boyce, B. F., Story, B., Wright, K. R., Chapman, M., Boyce, R., Mundy, G. R., and Yoneda, T. Bisphosphonate risedronate reduces metastatic human breast cancer burden in bone in nude mice. Cancer Res., *55:* 3551–3557, 1995.

23. Yoneda, T., Sasaki, A., Dunstan, C., Williams, P. J., Bauss, F., De Clerck, Y. A., and Mundy, G. R. Inhibition of osteolytic bone metastasis of breast cancer by combined treatment with the bisphosphonate ibandronate and tissue inhibitor of the matrix metalloproteinase-2. J. Clin. Investig., *99:* 2509–2517, 1997.

24. Peyruchaud, O., Winding, B., Pecheur, I., Serre, C. M., Delmas, P., and Clezardin, P. Early detection of bone metastases in a murine model using fluorescent human breast cancer cells: application to the use of the bisphosphonate zoledronic acid in the treatment of osteolytic lesions. J. Bone Miner. Res., *16:* 2027–2034, 2001.

25. Mundy, G. R., Yoneda, T., and Hiraga, T. Preclinical studies with zoledronic acid and other bisphosphonates: impact on the bone microenvironment. Semin. Oncol., *28:* 35–44, 2001.

26. Lee, M. V., Fong, E. M., Singer, F. R., and Guenette, R. S. Bisphosphonate treatment inhibits the growth of prostate cancer cells. Cancer Res., *61:* 2602–2608, 2001.

27. Luckman, S. P., Hughes, D. E., Coxon, F. P., Graham, R., Russell, G., and Rogers, M. J. Nitrogen-containing bisphosphonates inhibit the mevalonate pathway and prevent post-translational prenylation of GTP-binding proteins, including Ras. J. Bone Miner. Res., *13:* 581–589, 1998.

28. Coxon, F. P., Benford, H. L., Russell, R. G., and Rogers, M. J. Protein synthesis is required for caspase activation and induction of apoptosis by bisphosphonate drugs. Mol. Pharmacol., *54:* 631–638, 1998.

29. Shipman, C. M., Croucher, P. I., Russel, R. G. G., Helfrich, M. H., and Rogers, M. J. The bisphosphonate Incadronate (YM175) causes apoptosis of human myeloma cells *in vitro* by inhibiting the mevalonate pathway. Cancer Res., *58:* 5294–5297, 1998.

30. Teronen, O., Konttinen, Y. T., Lindqvist, C., Salo, T., Ingman, T., Lauhio, A., Ding, Y., Santavirta, S., Valleala, H., and Sorsa, T. Inhibition of matrix metalloproteinase-1 by dichloromethylene bisphosphonate (clodronate). Calcif. Tissue Int., *61:* 59–61, 1997.

31. Farina, A. R., Tacconelli, A., Teti, A., Gulino, A., and Mackay, A. R. Tissue inhibitor of metalloproteinase-2 protection of matrix metalloproteinase-2 from degradation by plasmin is reversed by divalent cation chelator EDTA and the bisphosphonate alendronate. Cancer Res., *58:* 2957–2960, 1998.

32. Ellis, W. J., Vessella, R. L., Buhler, K. R., Bladou, F., True, L. D., Bigler, S. A., Curtis, D., and Lange, P. H. Characterization of a novel androgen-sensitive, prostate-specific antigen-producing prostatic carcinoma xenograft: LuCaP 23. Clin. Cancer Res., *2:* 1039–1048, 1996.

33. Li, X., Traganos, F., Melamed, M. R., and Darzynkiewicz, Z. Single-step procedure for labeling DNA strand breaks with fluorescein- or BODIPY-conjugated deoxynucleotides: detection of apoptosis and bromodeoxyuridine incorporation. Cytometry, *20:* 172–180, 1995.

34. Poot, M., and Pierce, R. H. Detection of changes in mitochondrial function during apoptosis by simultaneous staining with multiple fluorescent dyes and correlated multiparameter flow cytometry. Cytometry, *35:* 311–317, 1999.

35. Quinn, J. E., Buhler, K. R., Brown, J. M., Bladou, F., Lange, P. H., and Vessella, R. L. A model of prostate cancer bone metastasis: Direct intra-bone injection of prostate cancer xenografts. J. Bone Miner. Res. *23* (Suppl. 597), 1998.

36. Lebeau, A., Muthmann, H., Sendelhofert, A., Diebold, J., and Lohrs, U. Histochemistry and immunohistochemistry on bone marrow biopsies. A rapid procedure for methyl methacrylate embedding. Pathol. Res. Pract., *191:* 121–129, 1995.

37. Skinner, R. A., Hickmon, S. G., Lumpkin, C. K., Aronson, J., and Nicholas, R. W. Decalcified bone: twenty years of successful specimen management. J. Histotechnology, *20:* 267–277, 1997.

38. Villanueva, A. R., and Mehr, L. A. Modifications of the Goldner and Gomori one-step trichrome stains for plastic-embedded thin sections of bone. Am. J. Med. Technol., *43:* 536–538, 1977.

39. Brown, L. G., Wegner, S. K., Wang, H., Buhler, K. R., Arfman, E. W., Lange, P. H., and Vessella, R. L. A novel monoclonal antibody (107–1A4) with high prostate specificity: generation, characterization of antigen expression, and targeting of human prostate cancer xenografts. Prostate Cancer Prostatic Disease, *1:* 208–215, 1998.

40. Corey, E., Quinn, J. E., Bladou, F., Brown, L. G., Roudier M. P, Brown, J. M., Buhler, K. R., and Vessella R. L. Establishment and characterization of osseous prostate cancer models: intra-tibial injection of human prostate cancer cells. Prostate, *52*: 2002.

41. Sato, M., Grasser, W., Endo, N., Akins, R., Simmons, H., Thompson, D. D., Golub, E., and Rodan, G. A. Bisphosphonate action. Alendronate localization in rat bone and effects on osteoclast ultrastructure. J. Clin. Investig., *88:* 2095–2105, 1991.

42. Luckman, S. P., Coxon, F. P., Ebetino, F. H., Russell, R. G. G., and Rogers, M. J. Heterocycle-containing bisphosphonates cause apoptosis and inhibit bone resorption by preventing protein prenylation: evidence from structure-activity relationships in J774 macrophages. J. Bone Miner. Res., *13:* 1668–1678, 1998.

43. Herrmann, J. L., Briones, F., Jr., Brisbay, S., Logothetis, C. J., and McDonnell, T. J. Prostate carcinoma cell death resulting from inhibition of proteasome activity is independent of functional Bcl-2 and p53. Oncogene, *17:* 2889–2899, 1998.

44. Burchardt, M., Burchardt, T., Shabsigh, A., Ghafar, M., Chen, M. W., Anastasiadis, A., de la, T. A., Kiss, A., and Buttyan, R. Reduction of wild type p53 function confers a hormone resistant phenotype on LNCaP prostate cancer cells. Prostate, *48:* 225–230, 2001.

45. Guise, T. A. Molecular mechanisms of osteolytic bone metastases. Cancer (Phila.), *88:* 2892–2898, 2000.

46. Zhang, J., Dai, J., Qi, Y., Lin, D. L., Smith, P., Strayhorn, C., Mizokami, A., Fu, Z., Westman, J., and Keller, E. T. Osteoprotegerin inhibits prostate cancer-induced osteoclastogenesis and prevents prostate tumor growth in the bone. J. Clin. Investig., *107:* 1235–1244, 2001.

47. Kafienah, W., Bromme, D., Buttle, D. J., Croucher, L. J., and Hollander, A. P. Human cathepsin K cleaves native type I and II collagens at the N-terminal end of the triple helix. Biochem. J., *331:* 727–732, 1998.

48. Littlewood Evans, A. J., Bilbe, G., Bowler, W. B., Farley, D., Wlodarski, B., Kokubo, T., Inaoka, T., Sloane, J., Evans, D. B., and Gallagher, J. A. The osteoclast-associated protease cathepsin K is expressed in human breast carcinoma. Cancer Res., *57:* 5386–5390, 1997.

49. Brubaker, K. D., Thomas, R., Vessella, R. L., and Corey, E. Cathepsin K mRNA and protein expression in prostate cancer progression. J. Bone Miner. Res., in press, 2003.

50. Teronen, O., Heikkila, P., Konttinen, Y. T., Laitinen, M., Salo, T., Hanemaaijer, R., Teronen, A., Maisi, P., and Sorsa, T. MMP inhibition and downregulation by bisphosphonates. Ann. N. Y. Acad. Sci., *878:* 453–465, 1999.

51. Nemeth, J. A., Yousif, R., Herzog, M., Che, M., Upadhyay, J., Shekarriz, B., Bhagat, S., Mullins, C., Fridman, R., and Cher, M. L. Matrix metalloproteinase activity, bone matrix turnover, and tumor cell proliferation in prostate cancer bone metastasis. J. Natl. Cancer Inst., *94:* 17–25, 2002.

JOURNAL OF BONE AND MINERAL RESEARCH
Volume 18, Number 2, 2003

Cathepsin K mRNA and Protein Expression in Prostate Cancer Progression*

KD BRUBAKER,[1] RL VESSELLA,[1,2] LD TRUE,[3] R THOMAS,[1] and E COREY[1]

ABSTRACT

Prostate cancer (CaP) is the most commonly diagnosed malignancy in men and is often associated with bone metastases, which cause much of the morbidity associated with CaP. Lesions associated with CaP generally exhibit increased bone formation and resorption. Increased bone resorption may release factors from the extracellular matrix that contribute to tumor growth. Cathepsin K (cat K) is a cysteine protease that exhibits strong degradative activity against the extracellular matrix and is involved in osteoclast-mediated bone destruction. In this study, we analyzed the expression of cat K in CaP cell lines and patient samples. Cat K message was detected in CaP cell lines by reverse transcription-polymerase chain reaction (RT-PCR) and in primary CaP and metastases by in situ hybridization. Immunohistochemistry revealed variable expression of cat K in primary CaP samples, as well as nonosseous metastases, whereas expression in bone metastases was significantly higher than in primary CaP, and normal prostate tissues were negative. Cat K protein was detected in CaP cell lines by Western blotting after immunoprecipitation. Cat K enzymatic activity was also detected in CaP cell lines by a fluorogenic assay and by an assay for degradation of collagen type I. Increased levels of NTx, a marker of bone matrix degradation mediated primarily by cat K, were also detected in sera of patients with CaP bone metastases. We hypothesize that CaP-expressed cat K may contribute to the invasive potential of CaP, while increased expression in bone metastases is consistent with a role in matrix degradation. (J Bone Miner Res 2003;18:222–230)

Key words: cathepsin K, prostate cancer, bone metastases, cysteine proteases

INTRODUCTION

BONE IS THE second most common site of metastasis (after lymph nodes) for prostate cancer (CaP). Although most CaP bone metastases are considered osteoblastic, based on patterns observed on radiographs, there is evidence that markers of bone resorption are elevated in patients with CaP bone lesions.[1–3] Detailed studies of bone metastases using histomorphometry have also demonstrated that radiographically sclerotic lesions exhibit both bone formation and resorption.[4–7] Recently it has been established that various cancers, including breast and prostate, support osteoclastogenesis through expression of the receptor activator of NF-kB ligand (RANKL),[8–10] providing one possible mechanism to explain the increased bone resorption observed with bone metastases. In addition to supporting osteoclast formation, it has been demonstrated that CaP expresses proteases that degrade matrix proteins, representing another potential mechanism of increased bone matrix degradation associated with bone metastases. In 1998, Sanchez-Sweatman et al.[11] reported that a CaP cell line, PC-3, degrades bone extracellular matrix and mineralized bone in vitro by secreting matrix metalloproteinases (MMPs). Nemeth et al.[12] demonstrated that MMP inhibitors prevented bone degradation in a PC-3-human bone-SCID mouse model. They observed that PC-3 tumors expressed MMPs in vivo, raising the possibility that the tumor cells participate in the process of bone turnover through expression of proteases.

Cathepsin K (cat K) is a cysteine protease secreted by osteoclasts that degrades extracellular matrix during bone resorption. Its significance in bone remodeling is demonstrated by the osteopetrotic phenotype observed in knockout studies.[13] Cat K has one of the highest matrix degradation

*This study was presented in part at the 92nd Annual Meeting of the American Association for Cancer Research, New Orleans, LA, March 24–28, 2001, and the 23rd Annual Meeting of the American Society for Bone and Mineral Research in Phoenix, AZ, October 12–16, 2001.

The authors have no conflict of interest.

[1]Department of Urology, University of Washington School of Medicine, Seattle, Washington, USA.
[2]Puget Sound VA Healthcare System, Seattle, Washington, USA.
[3]Department of Pathology, University of Washington School of Medicine, Seattle, Washington, USA.

activities known, cleaving type I collagen with higher efficiency than other cathepsins and MMPs, and its elastinolytic activity is higher than that of cat L and pancreatic elastase.[14,15] Because of its ability to destroy matrix components efficiently, cat K and some of its family members have been implicated in diseases involving bone and cartilage destruction, including tumor invasion[16–19] and rheumatoid arthritis.[20,21]

While its proteolytic activity is strongest at low pHs as in the lacunae of osteoclasts,[22] cat K can also degrade extracellular matrix components at neutral pHs, suggesting a general role in tissue destruction and remodeling.[23] In addition to the strong expression observed in osteoclasts, cat K protein has been detected in breast cancer,[24] sites of granulomatous inflammation,[25] human lung,[26] thyroid epithelial cells,[27] human endometrium,[28] and mouse ovary.[29]

In this study, we report detection of cat K message and protein in samples representing various stages of CaP progression and show that cat K expressed by CaP cells possesses enzymatic activity. Our data suggest that cat K derived from CaP cells may play a role in tumor invasiveness and extracellular bone matrix degradation.

MATERIALS AND METHODS

Tissue culture

CaP cell lines, DU 145, PC-3, B-PC-3, N-PC-3, LNCaP, C4, and C4–2 were cultured in RPMI-1640 medium (Life Technologies, Gaithersburg, MD, USA) supplemented with 10% FBS (Life Technologies) at 37°C under standard conditions. Murine osteoclasts were generated from bone marrow of Balb/c mice (Charles River, Hollister, CA, USA) as follows. Femur marrow cavities were flushed five to six times with phenol red-free MEM (Life Technologies), and cells were centrifuged at 500*g* and plated at a density of 1×10^6 cells per 9.6 cm^2 well. Cells were cultured in MEM supplemented with 2% FBS, 30 ng/ml colony-stimulating factor-1 (CSF-1; R&D Systems, Minneapolis, MN, USA), and 50 ng/ml RANKL (Chemicon, Temecula, CA, USA) for 5–6 days. Media was replaced every third day of culture. Osteoclast formation was confirmed by detection of TRACP+ multinucleated cells (TRACP assay, Sigma, St. Louis, MO, USA) after 5–6 days in culture, and the appearance of resorptive activity on dentine wafers (Immunodiagnostic Systems Ltd., Boldon, UK).

Tissue samples

Human prostate tissue samples used in this study were obtained from organ donors ($n = 2$), radical prostatectomies ($n = 16$), or rapid autopsies ($n = 14$). Tissues were fixed in 10% buffered formalin and embedded in paraffin. Bone samples were fixed in formalin and decalcified in 5% formic acid before embedding. Five-micrometer sections were used for immunohistochemistry (IHC) and in situ hybridization (ISH). Slides were baked at 60°C overnight before deparaffinization in xylene (×3) and rehydration in a series of 100%, 95%, and 70% ethanol (EtOH) rinses. Tissue integrity was assessed by hematoxylin and eosin staining, and the presence of CaP cells was assessed by prostate specific antigen (PSA) staining.

RT-PCR

Total RNA was isolated from CaP cell lines using STAT 60 (Tel-Test, Friendswood, TX, USA) according to the manufacturer's instructions. cDNA was generated from 1 μg total RNA using Moloney murine leukemia virus (MMLV) reverse transcriptase (Clontech, Palo Alto, CA, USA) with random hexamers. A 399-bp fragment of cat K (bps 906-1305, accession no. X82153) was amplified using primers: 5′-CAGCAAAGGTGTGTATTATGATGAAAGC and 3′-ATGGGTGGAGAGAAGCAAAGTAGGAAGG. $Beta_2$-microglobulin cDNA was amplified as a control for RNA quality, and polymerase chain reaction (PCR) conditions were as previously reported[30]: 1 cycle at 80°C for 3 minutes, and then 30–35 cycles of 94°C for 10 s, 69°C for 1 minute, and a final extension period at 72°C for 7 minutes.

ISH

The 399-bp amplicon of cat K was cloned into the pGEM-T vector (Promega, Madison, WI, USA). DNA sequencing was used to confirm the identity and determine the orientation of the insert. Purified plasmid was linearized using either *NcoI* or *NotI* and digoxigenin-labeled anti-sense and sense riboprobes were generated using a T7 and SP6 in vitro transcription kit (Roche, Indianapolis, IN, USA). The probes were separated on a 1.2% agarose gel, and relative amounts of RNA were quantified using a digital image analyzer (Alpha Innotech Corp., San Leandro, CA, USA). ISH was performed using the Ventana gen^{II} automated ISH system (Ventana Medical Systems, Tuscon, AZ, USA). Hybridization was performed using 25 ng/slide sense or anti-sense riboprobes at 45°C for 5 h in hybridization buffer (8 mM Tris, pH 8.0, 50% deionized formamide, 10% dextran sulfate, 1× Denhardt's solution, 0.3 M NaCl, 0.8 mM EDTA, 2 mg/ml yeast tRNA, 10.0 mM DTT), with subsequent rinses of 2×, 1×, 1× SSC buffer at 45°C. An anti-digoxigenin monoclonal antibody (1:2000; Sigma) was used with biotinylated rabbit anti-mouse antibodies, streptavidin-horseradish peroxidase (HRP), and diaminobenzidine (DAB) as the substrate. Sections were counterstained with Harris' hematoxylin before mounting.

IHC

Endogenous peroxidase was quenched by incubation of tissues in 0.3% hydrogen peroxide in PBS for 10 minutes. Nonspecific binding was blocked with serum block (5% goat, 5% horse, 5% rabbit sera) in PBS for 1 h at room temperature. Endogenous biotin was blocked using an avidin/biotin blocking kit (Vector Laboratories, Burlingame, CA, USA). An affinity purified chicken antibody against human cat K (Immunodiagnostic Systems Ltd.) was applied at 40 ng/ml, and the sections were incubated overnight at 4°C in a humidified chamber. Negative control sections were incubated with isotype-matched chicken IgY (Jackson ImmunoResearch Laboratories, West Grove, PA, USA). Sections were incubated with biotin-conjugated rabbit anti-chicken antibodies (1:250, Chemicon) for 30 minutes at room temperature and processed with an ABC kit (Vector Laboratories) with DAB. Sections were counterstained in Harris hematoxylin and blue in ammonia water

before mounting. Giant cell tumor tissues were used as a positive control for cat K staining.

Statistics for IHC samples

The percentage of cat K-positive cells in tissues was assessed as 0%, 1–25%, 25–50%, 50–75%, or 75–100% by a pathologist, who was blinded to the samples, and assigned values of 0, 1, 2, 3, or 4, respectively. Immunoreactivity in primary CaP and nonosseous and osseous metastases were compared using a one-way ANOVA with a Bonferroni's comparison posttest.

Immunoprecipitation of cat K

Approximately 500 μg CaP tissue or 5×10^6 LNCaP or PC-3 cells were homogenized in 1.0 ml lysis buffer (10 mM Tris, pH 7.4, 50 mM NaCl, 0.25% Triton X-100, 0.25% sodium deoxycholate, 0.5% CHAPS, and Complete protease inhibitors) and centrifuged for 20 minutes at 14,000 rpm before immunoprecipitation. Cat K protein was immunoprecipitated overnight at 4°C using a mixture of mouse monoclonal anti-cat K antibodies CP1A240.2 and CP1K338.4 (0.25 mg each, a gift from Beckman Coulter Inc., Fullerton, CA, USA), which were bound to protein G Sepharose beads (Pierce, Rockford, IL, USA). After extensive washes to release unbound proteins, cat K was eluted from the column as recommended by the manufacturer. The eluted protein was separated on a 15% SDS-PAGE gel and transferred to polyvinylidene difluoride (PVDF) at 100 V for 1 h. Cat K protein was detected using a mouse monoclonal antibody CP1A713 (0.25 μg/ml, a gift from Beckman Coulter Inc.). MOPC21 (Sigma), an unrelated mouse monoclonal antibody, was used as a negative control. Blots were incubated with goat anti-mouse-HRP conjugated secondary (1:3000; Santa Cruz Biotechnology Inc., Santa Cruz, CA, USA) antibody and Amersham ECL (Piscataway, NJ, USA) was used for detection with Kodak X-OMAT AR film (Rochester, NY, USA).

Cleavage of Z-GPR-MCA

After tissue culture (see above) CaP cells ($\sim 1–3 \times 10^6$) or osteoclasts (Oc, $\sim 10^5$) were lysed in 1.0 ml assay buffer (50 mM sodium acetate, pH 5.5, 2.5 mM dithiothreitol and 2.5 mM EDTA) on ice containing 1.0% Triton X-100. Protein levels were determined using the Bio-Rad DC protein assay kit (Bio-Rad, Hercules, CA, USA). One hundred microliters lysate (corresponding to 150–200 μg protein for CaP cell lines and 5–10 μg for osteoclasts) was added to 400 μl assay buffer, or buffer containing either a general cysteine protease inhibitor E64 (L-trans-epoxy-succinyl-Leu-4-guanidinobutylamide; Calbiochem, San Diego, CA, USA) or a cathepsin B inhibitor, CA 074 (L-trans-epoxy-succinyl-Ile-Pro-OH propylamide; Calbiochem). Reaction tubes were incubated for 30 minutes at room temperature before the addition of 10 μl of 4×10^{-3} M Z-GPR-MCA (benzyloxycarbonyl-Gly-Pro-Arg-7-amido-4-methylcoumarin, 80 μM final concentration; Bachem, King of Prussia, PA, USA). The reactions were placed at 37°C (10 minutes for Oc, 30 minutes for LNCaP and DU 145, and 75 minutes for PC-3) and terminated by addition of 500 μl of stopping reagent (100 mM sodium monochloroacetate, 30 mM sodium acetate, 70 mM acetic acid, pH 4.3). Cleavage of the substrate was measured by the fluorescent emission of the free aminomethylcoumarin at 470 nm (excitation, 360 nm). A standard curve was generated with 7-amino-4-methylcoumarin (0.01–5 μM) to calculate the amount of coumarin released. Human liver cathepsin B (200 ng, Calbiochem) was used to determine the dose response to CA 074.

Type I collagen degradation assay

Lysates from PC-3, LNCaP, DU 145, and osteoclasts (200 μl total volume, 150 μg protein; 10 μg for Oc), prepared in the same assay buffer used in the Z-GPR-MCA experiments, were added to wells in a 96-well plate coated with 1.2 μg/ml purified rat type I *N*-[propionate-2,3-^{3}H]propionylated collagen (NEN Life Science Products, Boston, MA, USA). After a 6-h incubation at 37°C, 75 μl of the reaction was collected, 3 ml CytoScint scintillation cocktail (ICN, Costa Mesa, CA, USA) was added, and release of degradation products of collagen was measured using a Beckman LS-3801 beta spectrometer (Beckman Coulter Inc.). Lysates were also treated with E64 (1 μM) to inhibit cysteine protease activity. Samples were run in triplicate in three separate experiments. The experimental data are presented as the mean ± SEM of the three sets, which have been normalized to the maximum signal strength. Statistical significance between untreated and 1-μM E64 samples was determined by unpaired *t*-tests.

Bone resorption pit assay

LNCaP and PC-3 (50,000 cells/well) were cultured on dentine wafers (Immunodiagnostic Systems Ltd.) in 24-well plates with 1 ml RPMI 1640 + 10% FBS. Osteoclasts, generated as described in the tissue culture section, were used as a positive control for resorption. After 5–6 days of culture, the media was removed and replaced with 1 M NH_4OH for 30 minutes. The dentine wafers were then cleaned by ultrasonication for 30 minutes and stained with hematoxylin (Zymed, South San Francisco, CA, USA) for 1 minute and washed with distilled water. Resorption pits were visualized under transmitted light.

N-telopeptides of type I collagen ELISA

Cross linked N-telopeptides of type I collagen (NTx) were measured in serum samples from CaP patients using the Osteomark assay kit (Ostex International Inc., Seattle, WA, USA). Serum samples were obtained from 10 donors (mean PSA = 1.09 ± 0.16); 10 patients with organ-confined CaP, stages T_{2a-c} or T_{1c} (mean PSA = 7.43 ± 1.16); 5 patients with bone metastases who had not received any treatment (mean PSA = 557.6 ± 173.3); 8 patients with bone metastases who had received one or more treatments for CaP, including androgen ablation, chemotherapy or radiation (mean PSA = 1087 ± 464); and 6 patients who had received bone resorption inhibitors in addition to other treatments listed above (mean PSA = 4097 ± 1729). All patients gave informed consent. The majority of the patients used for this assay were the same patients used in the ISH and IHC studies. NTx levels were compared for statistical significance using a one-way ANOVA with a Bonferroni's comparison posttest.

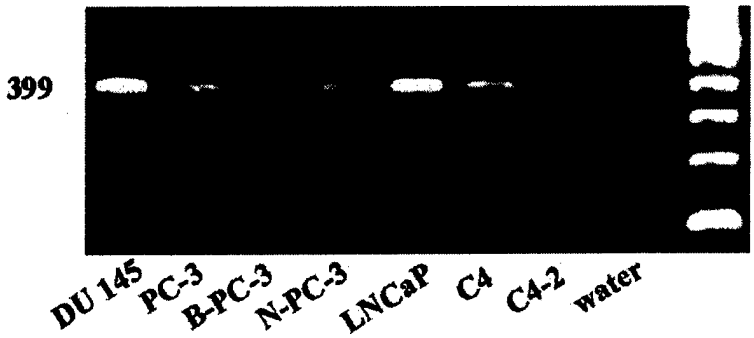

FIG. 1. Detection of cat K message in CaP by RT-PCR. The 399-bp amplicon was detected in DU 145, PC-3, sublines B-PC-3 and N-PC-3, LNCaP, and sublines C4 and C4–2.

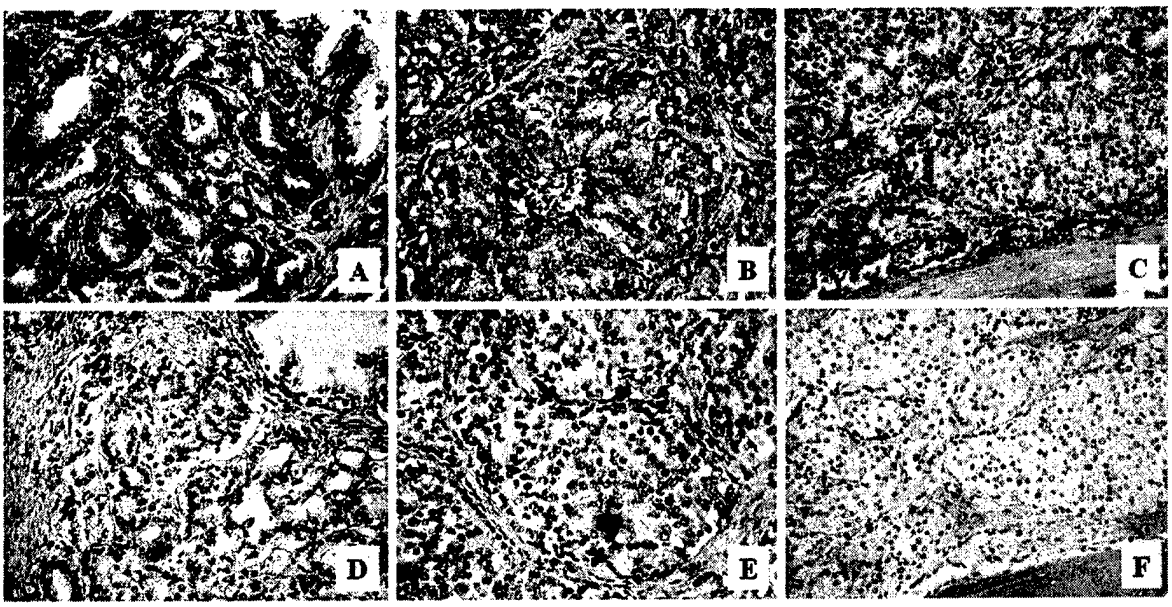

FIG. 2. Localization of cat K mRNA in CaP tissues by in situ hybridization. Representative samples of localized CaP demonstrated cat K message in (A) secretory epithelial cells and occasionally in basal and luminal cells of normal glands (arrowhead, A). Cat K message was also detected in (B) CaP metastases, such as the lymph node (LN) metastasis, and (C) the osseous metastasis. (D–F) The sense controls for each tissue. Magnification, ×50.

RESULTS

Expression of cat K mRNA

Cat K mRNA was detected in all CaP cell lines tested, which include the androgen-independent cell lines DU 145 and PC-3, the PC-3 sublines, B-PC-3 and N-PC-3, the androgen-sensitive cell line LNCaP, and its androgen-independent sublines C4 and C4–2 by RT-PCR (Fig. 1). In addition, the presence of cat K mRNA was assessed in 2 samples of normal prostate from organ donors, 7 localized CaP tumors, and 25 metastatic samples from 7 patients by ISH. ISH demonstrated the presence of cat K mRNA in epithelial cells of primary CaP in 5 of 7 samples (Fig. 2A), while a moderate signal was observed in basal and luminal cells of normal glands (3/7, Fig. 2A, arrow) adjacent to the cancer. Samples of normal prostate from organ donors were negative. Cat K mRNA was detected in nonosseous metastases including liver (2/2), lymph node (2/3, Fig. 2B), and lung (1/1), and 15/19 osseous CaP metastases (Fig. 2C). When present, osteoclasts were intensely positive for cat K message. Cat K mRNA was not observed in stromal fibroblasts, stromal smooth muscle, or vascular smooth muscle. Staining with the sense probe was negative (Figs. 2D–2F).

Cat K protein expression in CaP

The presence of cat K protein was assessed in 14 samples of localized CaP and in 52 metastases from 14 patients. Immunohistochemistry revealed the presence of cat K protein in the epithelial cells of cancerous glands in 6/14 primary CaP samples (Fig. 3A). Normal glands adjacent to CaP were negative. Cat K protein was also detected in metastases to liver (3/4), lung (3/3), adrenal (1/1), and lymph node (4/10, Fig. 3B); however the immunoreactivity in these samples was variable, ranging from no staining to 100% positivity. Osseous metastases were positive for cat K protein expression in 30/34 samples (Fig. 3C). Intense immunoreactivity for cat K was observed in osteoclasts in CaP bone metastases (Fig. 3C, arrow). A giant cell tumor was

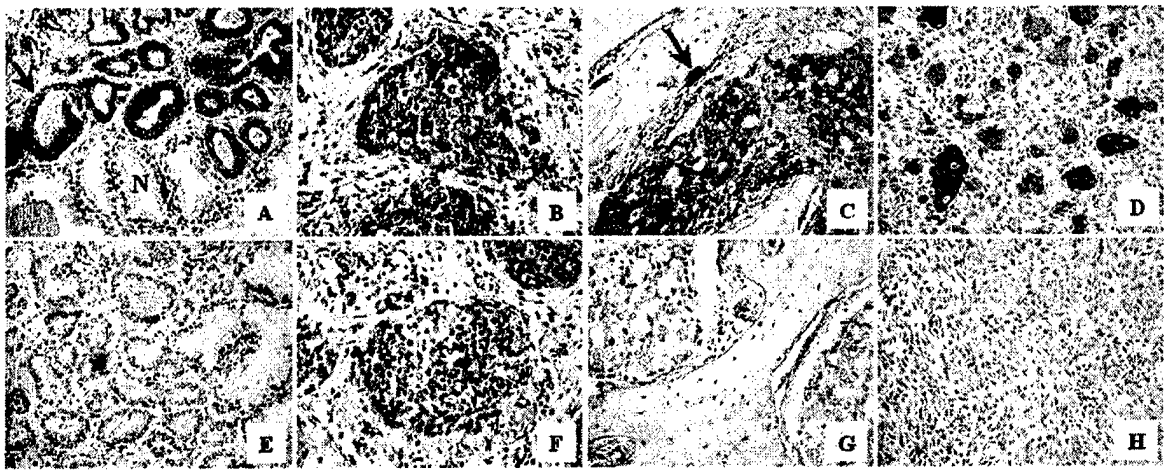

FIG. 3. Immunolocalization of cat K protein in CaP tissues. Cat K protein was detected in (A) cancerous glands (arrow) of ~ 40% of the patients tested, whereas normal glands (N) were negative. CaP metastases were generally positive for cat K protein as observed in (B) the LN metastasis and (C) the bone metastasis. Osteoclasts in bone metastases were also strongly positive (arrow, C). (D) Giant cell tumor was used as a positive control for cat K immunoreactivity. (E–H) The negative control sections. Magnification, ×50.

used as the positive control for cat K staining (Fig. 3D). Table 1 summarizes IHC results for metastases from nine patients in which multiple metastatic sites were evaluated. The percentage of tumor cells exhibiting cat K immunoreactivity in osseous metastases was significantly higher than in primary CaP ($p < 0.05$) and nonosseous ($p < 0.001$) samples. The percentages of tumor cells exhibiting cat K immunoreactivity in primary CaP versus nonosseous metastases were not significantly different ($p > 0.05$).

To confirm the presence of cat K protein in CaP, we performed Western blot analysis of cell lysates from CaP cell lines LNCaP and PC-3, and CaP tissues that were positive by IHC. We were unable to detect the cat K protein under these conditions. Therefore, we immunoprecipitated cat K from CaP cells lines and CaP tissues to obtain more concentrated samples. After this, a 40-kDa band was labeled in blots from CaP tissues (Fig. 4A, arrow) and LNCaP and PC-3 cell lines (Fig. 4B, arrow). The 40-kDa protein is most likely the proform of cat K.[23,31] The light chain band in Fig. 4B would be expected to mask the active form of cat K band at 28 kDa, but when non-denaturing gels were run as in Fig. 4A, we still did not observe a band at 28 kDa.

Cat K enzymatic activity

The presence of cat K enzymatic activity in CaP cells was evaluated using Z-GPR-MCA, a substrate that is highly selective for cat K versus cathepsins L and S.[23,31] Z-GPR-MCA cleavage activity was detected in LNCaP, PC-3, and DU 145 cell lines (Table 2). Because cathepsin B (cat B) also cleaves Z-GPR-MCA, but at a much lower rate, the portion of the activity caused by cat B was determined using the cat B inhibitor CA 074. CA 074 blocked approximately 75% of the activity in LNCaP and DU 145, and 50% of the activity in PC-3. The remaining activity was inhibited by a general cysteine protease inhibitor, E64, suggesting that it was caused by cat K. For inhibition of cat B activity, we used 50 nM CA 074, a concentration determined from dose-response experiments. Fifty nanomolar CA 074 inhibited purified human cat B activity with the Z-GPR-MCA substrate and a specific cat B substrate, Z-RR-MCA (data not shown) as effectively as E64. LNCaP and DU 145 exhibited 2.5- to 3-fold more Z-GPR-MCA cleavage activity than PC-3 after inhibition of cat B. Activity of cat K in osteoclast lysates, which were used as the positive control, was approximately 50-fold higher (normalized to protein) than in the LNCaP and DU 145 CaP cell lines. Because our osteoclast purity was 30–50% as determined by TRAP staining, the cat B activity in this preparation is most likely caused by contaminating mononuclear cells, because osteoclasts express low levels of cat B.[32,33]

We have also evaluated whether CaP cells exhibit pitting activity using dentine wafers. We were unable to detect pitting capabilities of CaP cells; osteoclasts were used as a positive control (data not shown). Because cat K can degrade type I collagen, we also performed experiments to determine whether CaP cells can degrade collagen. We observed type I collagen-degradation activity in LNCaP, DU 145, and osteoclast lysates under the same assay conditions used in the Z-GPR-MCA assay (Fig. 5). PC-3 lysates were unable to degrade collagen under the conditions used. The general cysteine protease inhibitor E64 blocked approximately 50% of the cleavage activity in LNCaP, DU 145, and osteoclast lysates, confirming that the activity is attributable to cysteine proteases.

NTx levels in sera from CaP patients

Increased type I collagen degradation associated with CaP bone metastases was demonstrated by measuring NTx levels in the sera of patients with either organ-confined CaP or CaP bone metastases (Fig. 6). The levels in patients with bone metastases who received treatment for CaP, including androgen ablation, which has been reported to increase bone resorption,[34,35] were statistically significant from the normal donors ($p < 0.001$) and primary CaP ($p < 0.01$; Table

TABLE 1. CAT K IHC RESULTS FOR CaP METASTASES OF NINE PATIENTS

Patient	*Tissue metastasis*	*% Positive*
1	Bone	0
	Bone	25–50
	Adrenal	50–75
	Lymph node	0
	Liver	50–75
2	Bone	1–25
	Bone	50–75
	Lymph node	0
	Lymph node	0
3	Bone	50–75
	Bone	50–75
	Bone	75–100
	Bone	75–100
	Lymph node	1–25
4	Bone	75–100
	Bone	75–100
	Bone	75–100
	Lymph node	75–100
	Liver	75–100
5	Bone	75–100
	Bone	50–75
	Bone	75–100
	Lung	1–25
	Lymph node	0
	Lymph node	0
6	Bone	25–50
	Lymph node	75–100
	Lymph node	25–50
	Liver	75–100
7	Bone	75–100
	Bone	50–75
	Lung	50–75
8	Bone	25–50
	Liver	0
9	Bone	1–25
	Lung	25–50

The percentage of cat K positive CaP in multiple metastases from nine patients are presented.

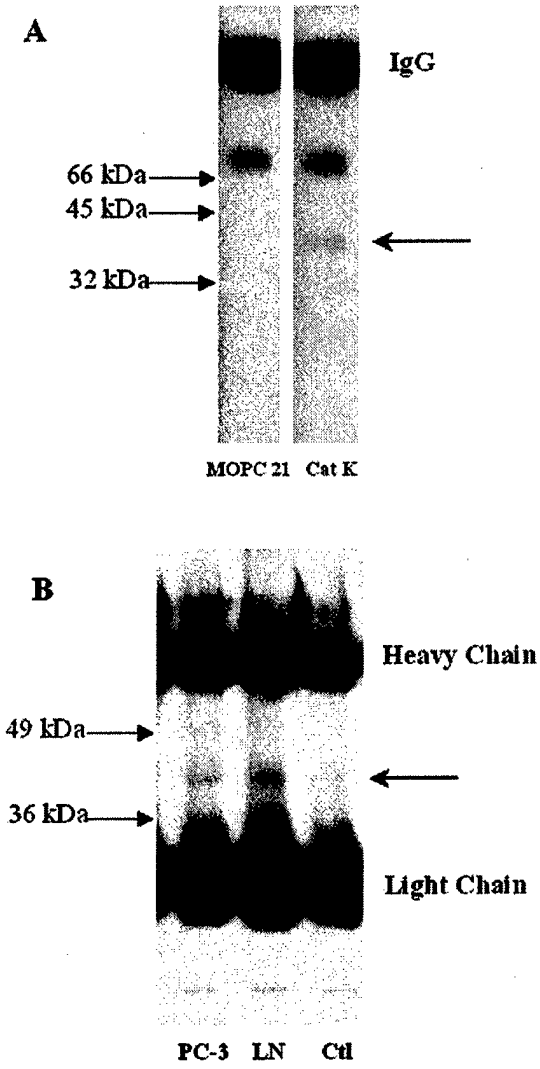

FIG. 4. Immunoprecipitation of cat K from CaP tissues and cell lines. (A) Cat K was immunoprecipitated from a pool of CaP tissues and run on a 15% non-denaturing SDS-PAGE gel. After transfer to PVDF, the blot was probed for cat K with antibody clone, CP1A713. A 40-kDa band was labeled (arrow), corresponding to the size of the proform of cat K. A control mouse antibody, MOPC 21, was used to label the same samples. The immunoprecipitating IgG is labeled, and molecular weight markers are noted to the left of the blot. (B) Cat K was immunoprecipitated from LNCaP (LN) and PC-3 cell lysates and run on a 12% SDS-PAGE denaturing gel and transferred to PVDF. A 40-kDa band (arrow) was also detected. A control reaction (Ctl) was also run, in which LNCaP cell lysate was incubated with mouse IgG. The heavy and light chains of the antibody are labeled.

3). NTx levels in patients with bone metastases who were not treated for CaP were statistically significant from the normal controls ($p < 0.05$).

DISCUSSION

In this study, we present data suggesting that cat K, a cysteine protease normally associated with osteoclastic bone resorption, is associated with CaP progression. The presence of cat K in primary CaP is consistent with a possible role in matrix degradation via digestion of type I collagen, before dissociation and dissemination. However, the same enzymatic activity at metastatic sites in the bone may promote establishment of micrometastases and may also lead to release of factors supporting tumor growth.

We observed cat K protein in cancerous glands of approximately 40% of the primary CaP tissues tested, exhibiting no correlation with Gleason score or cancer grade. Although prostate basement membrane consists primarily of type IV collagen[36,37] and laminin,[38,39] Burns-Cox et al.[40] observed an increase in type I collagen synthesis and degradation at the cancer foci in biopsy specimens from patients with primary CaP. Enzymes that cleave type I collagen, such as the cathepsins and MMPs, are reported to be upregulated in CaP.[17,41–46] Therefore, cat K may be an important factor at the local level in CaP dissemination. However, we did not detect a significant increase in NTx levels in CaP patients with organ-confined disease versus control samples. A possible explanation is that the levels of

TABLE 2. CAT K CLEAVAGE ACTIVITY IN PROSTATE CANCER CELL LINES AND OSTEOCLASTS

	Activity	*CA 074 (50 nM)*	*E64 (1 μM)*
Osteoclasts	7.59 ± 0.64	1.88 ± 0.43	0.581 ± 0.36
LNCaP	0.150 ± 0.053	0.038 ± 0.010	0.017 ± 0.006
DU 145	0.115 ± 0.045	0.029 ± 0.006	0.011 ± 0.002
PC-3	0.024 ± 0.005	0.012 ± 0.004	0.009 ± 0.003
Human cat B	0.704 ± 0.067	0.110 ± 0.017	0.093 ± 0.015

Cat K activity was measured in CaP cell lines, LNCaP, DU 145, and PC-3 using Z-GPR-MCA. Osteoclasts generated from mouse bone marrow were used as a positive control. CA 074 (50 nM) blocks cat B activity and E64 (1 μM) blocks all cysteine protease activity. Purified human cat B was also used to demonstrate the effectiveness of the CA 074 inhibition. Activity units, nmol Z-GPR-MCA cleaved/min/mg protein.

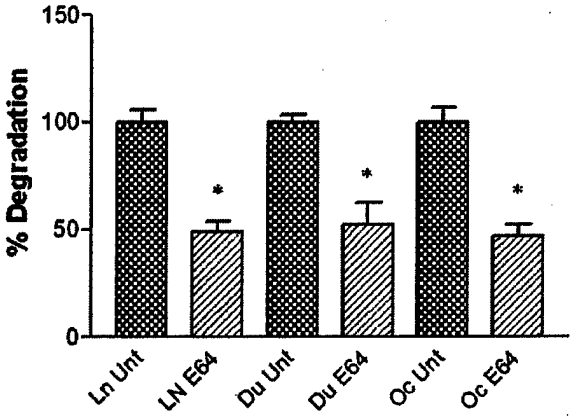

FIG. 5. Type I collagen degradation activity in LNCaP, DU 145, and osteoclast lysates. LNCaP (Ln), DU 145 (Du), and osteoclast (Oc) lysates released radiolabeled type I collagen fragments from coated wells at 37°C for 6 h. The percentage degradation activity was calculated by normalizing the counts per minute data, where untreated (Unt) samples = 100% activity. Data are presented as the mean ± SE from three experiments. E64 inhibited ~50% activity in all three cell lysates. The E64 data were statistically significant from the untreated samples as noted by the asterisk ($p < 0.0001$ [Ln], 0.0004 [Du], and 0.0001 [Oc]).

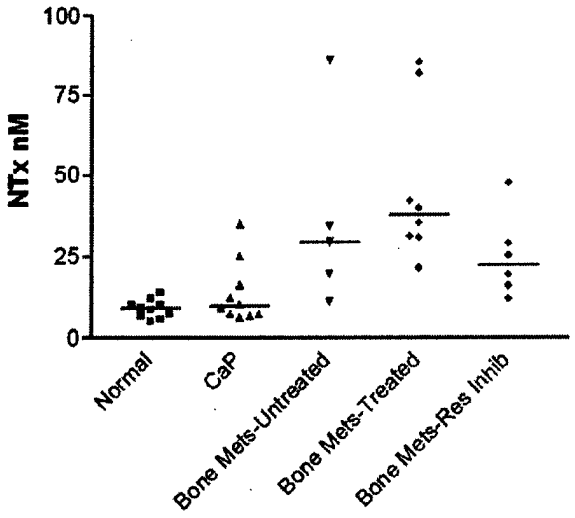

FIG. 6. Scatterplot of NTx levels in sera from normal donors and CaP patients. NTx levels (nM) were measured in sera from normal donors and CaP patients with either organ-confined CaP, bone metastases (mets) without treatments (untreated), bone mets with treatments (treated), or bone mets with bone resorption inhibitor (res inhib) treatment in addition to other treatments, which include androgen ablation, chemotherapy, or radiation. The horizontal bars represent the median of each group. NTx levels in untreated and treated patients with bone mets were statistically significant from the normal controls ($p < 0.05$ and $p < 0.001$, respectively), and the treated patients with bone mets were also significantly different from patients with primary CaP ($p < 0.01$).

TABLE 3. NTx LEVELS IN NORMAL DONORS AND PATIENTS WITH ORGAN-CONFINED CaP OR CaP BONE METASTASES

Group	*Number of patients*	*NTx levels (nM)*
Normal donors	10	9.10 ± 0.86
Organ-confined primary CaP	10	13.8 ± 2.97
Bone metastases—untreated	5	36.3 ± 13.1*
Bone metastases—treated	8	46.2 ± 8.52†‡
Bone metastases—bone resorption inhibitors	6	25.01 ± 5.20

NTx levels were measured in sera of normal donors or patients with organ-confined CaP or CaP bone metastases. Patients with bone metastases were subgrouped based on whether they received treatment for CaP or not and whether they also received bone resorption inhibitors.

* Statistical significance from normal donors, $p < 0.05$.

† Statistical significance from normal donors, $p < 0.001$.

‡ Statistical significance from organ-confined primary CaP, $p < 0.01$.

cat K and type I collagen in organ-confined CaP are insufficient to cause detectable systemic increases the of NTx levels. In the absence of long-term follow-up information on these patients, it is not possible to determine whether the presence of cat K in the primary tumor is strongly correlated with subsequent metastasis, but it is at least conceivable that this enzyme is important or even essential for dissemination of CaP cells from the primary tumor. This hypothesis is supported by the observation that metastases in general exhibited equal or higher positivity than the primary tumors (41/52).

We also observed higher cat K immunoreactivity in osseous metastases versus nonosseous and primary CaP. This is consistent with the NTx assay results, which demonstrated increased matrix degradation in patients with bone metastases versus normal controls and patients with primary CaP. Type I collagen is the major extracellular matrix component of bone, and there is an extensive body of evidence that type I collagen breakdown products, including NTx, are present at elevated levels in the serum and urine of patients with CaP bone metastases.[1–3,47–49] Increased resorption associated with bone metastases, including CaP bone metastases, is linked to stimulation of osteoclastogenesis through RANKL expression.[8–10] Augmented NTx levels are generally associated with increased osteoclastic bone resorption activity because of cat K expressed by these cells, yet we observed osteoclasts in samples from only 3/14 patients with advanced CaP bone metastases. Although we

sample 20 bone sites per patient, it is possible that we missed areas with extensive bone resorption and osteoclasts. Alternatively, the increased NTx levels may be in part because of the breakdown of type I collagen by cells other than osteoclasts, such as the CaP cells expressing cat K.

Detection of cat K mRNA and protein in CaP tissues and cell lines led us to determine whether the enzyme was catalytically active. We observed that LNCaP and DU 145 had 2.5- to 3-fold more activity than PC-3, whereas osteoclasts exhibited 50-fold more activity than LNCaP and DU 145 CaP cells in assays of Z-GPR-MCA cleavage. We also determined that LNCaP and DU 145 lysates exhibit type I collagen-degradation activity, whereas PC-3 do not. When CaP cells were plated on labeled collagen or dentine wafers, cleavage activity was not detected, although osteoclasts exhibited activity. Our activity data suggest that CaP cell lines in vitro express low levels of cat K, which seem not to be active in culture but can be activated at a low pH in lysates. The low levels of cat K activity in CaP cells correlated with our Western blotting/immunoprecipitation results: we detected a faint 40-kDa protein, corresponding to the proform of the enzyme.[23,31] We were unable to detect the 28-kDa active form of cat K, possibly because the quantity immunoprecipitated was below the level of detection. In addition, the presence of cystatins, natural inhibitors of the cathepsins, in CaP cell lines may also contribute to the low activity observed or difficulty in immunoprecipitation.[50] It is intriguing that PC-3 cells had lower levels of cat K activity than LNCaP, because PC-3 metastases in bone are osteolytic,[12,51] whereas LNCaP lesions exhibit both bone formation and resorption.[51] PC-3 express MMPs,[12] urokinase plasminogen activator,[52] RANKL,[53] endothelin-1,[54] and PTHrP[55]—factors involved in metastases to bone and bone remodeling. The formation of PC-3 osteolytic bone metastases seems to involve a complex set of mechanisms, and cat K may play a very minor role in this case. Moreover, the low cat K activity in CaP cell lines may not be representative of the expression or activity levels in CaP in vivo.

In this study we report our observations of the expression of cat K mRNA and protein in CaP cell lines and tissues, as well as cat K activity in CaP cell lines. The presence of cat K in primary CaP may promote the process of dissemination, whereas in osseous metastases, which exhibit higher levels of markers of bone formation and resorption, cat K is most likely involved in degradation of the extracellular matrix. This process may not only provide sites for CaP cell anchorage, but also cause the release of growth factors essential for tumor growth. Inhibition of cat K activity in vivo using xenograft models may permit a more precise definition of the role of CaP-expressed cat K and yield insight regarding novel therapeutic strategies.

ACKNOWLEDGMENTS

We would like to thank Beckman Coulter Inc. for generously providing us with the three monoclonal antibodies against cat K used in the immunoprecipitation/Western blotting experiments. We would also like to thank Lisha Brown for her expertise in tissue culture and Dr Michael Corey for editorial assistance. Support for this work was provided by National Institutes of Health Training Grant 5T32DK07779-02, NIDDK O'Brien Center Award DK47656-08, U.S. Army DOD DAMD17-00-1-0529, a Merit Review grant from the Department of Veterans Affairs, the Richard M. Lucas Foundation, and the CaPCure Foundation.

REFERENCES

1. Wymenga LF, Groenier K, Schuurman J, Boomsma JH, Elferink RO, Mensink HJA 2001 Pretreatment levels of urinary deoxypyridinoline as a potential marker in patients with prostate cancer with or without bone metastasis. Brit J Urol Int **88:**231–235.
2. Tamada T, Sone T, Tomomitsu T, Jo Y, Tanaka H, Fukunaga M 2001 Biochemical markers for the detection of bone metastasis in patients with prostate cancer: Diagnostic efficacy and the effect of hormonal therapy. J Bone Miner Metab **19:**45–51.
3. Noguchi M, Noda S 2001 Pyridinoline cross-linked carboxyterminal telopeptide of type I collagen as a useful marker for monitoring metastatic bone activity in men with prostate cancer. J Urol **166:** 1106–1110.
4. Charhon SA, Chapuy MC, Delvin EE, Valentin-Opran A, Edouard CM, Meunier PJ 1983 Histomorphometric analysis of sclerotic bone metastases from prostatic carcinoma special reference to osteomalacia. Cancer **51:**918–924.
5. Clarke NW, McClure J, George NJ 1991 Morphometric evidence for bone resorption and replacement in prostate cancer. Br J Urol **68:**74–80.
6. Scher HI, Chung LW 1994 Bone metastases: Improving the therapeutic index. Semin Oncol **21:**630–656.
7. Roudier MP, Higano C, True L, Ott S, Penson D, Vessella R, Lange P 2001 Concordance between bone histology and technitium 99 methylene diophosphonate bone scan in advanced prostate cancer patients with special reference to bisphosphonate treatment. Cancer Res **42:**793.
8. Chikatsu N, Takeuchi Y, Tamura Y, Fukumoto S, Yano K, Tsuda E, Ogata E, Fujita T 2000 Interactions between cancer and bone marrow cells induce osteoclast differentiation factor expression and osteoclast-like cell formation in vitro. Biochem Biophys Res Commun **267:**632–637.
9. Zhang J, Dai J, Qi Y, Lin DL, Smith P, Strayhorn C, Mizokami A, Fu Z, Westman J, Keller ET 2001 Osteoprotegerin inhibits prostate cancer-induced osteoclastogenesis and prevents prostate tumor growth in the bone. J Clin Invest **107:**1235–1244.
10. Mancino AT, Klimberg VS, Yamamoto M, Manolagas SC, Abe E 2001 Breast cancer increases osteoclastogenesis by secreting M-CSF and upregulating RANKL in stromal cells. J Surg Res **100:**18–24.
11. Sanchez-Sweatman OH, Orr FW, Singh G 1998 Human metastatic prostate PC3 cell lines degrade bone using matrix metalloproteinases. Invasion Metastasis **18:**297–305.
12. Nemeth JA, Yousif R, Herzog M, Che M, Upadhyay J, Shekarriz B, Bhagat S, Mullins C, Fridman R, Cher ML 2002 Matrix metalloproteinase activity, bone matrix turnover, and tumor cell proliferation in prostate cancer bone metastasis. J Natl Cancer Inst **94:**17–25.
13. Saftig P, Hunziker E, Wehmeyer O, Jones S, Boyde A, Rommerskirch W, Moritz JD, Schu P, von Figura K 1998 Impaired osteoclastic bone resorption leads to osteopetrosis in cathepsin-K-deficient mice. Proc Natl Acad Sci USA **95:**13453–13458.
14. Chapman HA, Riese RJ, Shi GP 1997 Emerging roles for cysteine proteases in human biology. Annu Rev Physiol **59:**63–88.
15. Garnero P, Borel O, Byrjalsen I, Ferreras M, Drake FH, McQueney MS, Foged NT, Delmas PD, Delaisse JM 1998 The collagenolytic activity of cathepsin K is unique among mammalian proteinases. J Biol Chem **273:**32347–32352.
16. Sinha AA, Wilson MJ, Gleason DF, Reddy PK, Sameni M, Sloane BF 1995 Immunohistochemical localization of cathepsin B in neoplastic human prostate. Prostate **26:**171–178.
17. Szpaderska AM, Frankfater A 2001 An intracellular form of cathepsin B contributes to invasiveness in cancer. Cancer Res **61:** 3493–3500.
18. Castiglioni T, Merino MJ, Elsner B, Lah TT, Sloane BF, Emmert-Buck MR 1994 Immunohistochemical analysis of cathepsins D. B, and L in human breast cancer. Hum Pathol **25:**857–862.
19. Yan S, Sameni M, Sloane BF 1998 Cathepsin B and human tumor progression. Biol Chem **379:**113–123.

20. Hummel KM, Petrow PK, Franz JK, Muller-Ladner U, Aicher WK, Gay RE, Bromme D, Gay S 1998 Cysteine proteinase cathepsin K mRNA is expressed in synovium of patients with rheumatoid arthritis and is detected at sites of synovial bone destruction. J Rheumatol **25**:1887–1894.
21. Dodds RA, Connor JR, Drake FH, Gowen M 1999 Expression of cathepsin K messenger RNA in giant cells and their precursors in human osteoarthritic synovial tissues. Arthritis Rheum **42**:1588–1593.
22. Littlewood-Evans A, Kokubo T, Ishibashi O, Inaoka T, Wlodarski B, Gallagher JA, Bilbe G 1997 Localization of cathepsin K in human osteoclasts by in situ hybridization and immunohistochemistry. Bone **20**:81–86.
23. Buhling F, Gerber A, Hackel C, Kruger S, Kohnlein T, Bromme D, Reinhold D, Ansorge S, Welte T 1999 Expression of cathepsin K in lung epithelial cells. Am J Respir Cell Mol Biol **20**:612–619.
24. Littlewood-Evans AJ, Bilbe G, Bowler WB, Farley D, Wlodarski B, Kukubo T, Inaoka T, Sloane J, Evans DB, Gallagher JA 1997 The osteoclast-associated protease cathepsin K is expressed in human breast carcinoma. Cancer Res **57**:5386–5390.
25. Diaz A, Willis AC, Sim RB 2000 Expression of the proteinase specialized in bone resorption, cathepsin K, in granulomatous inflammation. Mol Med **6**:648–659.
26. Buhling F, Waldburg N, Gerber A, Hackel C, Kruger S, Reinhold D, Bromme D, Weber E, Ansorge S, Welte T 2000 Cathepsin K expression in human lung. Adv Exp Med Biol **477**:281–286.
27. Tepel C, Bromme D, Herzog V, Brix K 2000 Cathepsin K in thyroid epithelial cells: Sequence, localization and possible function in extracellular proteolysis of thyroglobulin. J Cell Sci **113**: 4487–4498.
28. Jokimaa V, Oksjoki S, Kujari H, Vuorio E, Anttila L 2001 Expression patterns of cathepsins B. H, K, L and S in the human endometrium. Mol Hum Reprod **7**:73–78.
29. Oksjoki S, Soderstrom M, Vuorio E, Anttila L 2001 Differential expression patterns of cathepsins B. H, K, L and S in the mouse ovary. Mol Hum Reprod **7**:27–34.
30. Corey E, Arfman EW, Liu AY, Vessella RL 1997 Improved reverse transcriptase-polymerase chain reaction protocol with exogenous internal competitive control for prostate-specific antigen mRNA in blood and bone marrow. Clin Chem **43**:443–452.
31. Aibe K, Yazawa H, Abe K, Teramura K, Kumegawa M, Kawashima H, Honda K 1996 Substrate specificity of recombinant osteoclast-specific cathepsin K from rabbits. Biol Pharm Bull **19**:1026–1031.
32. Drake FH, Dodds RA, James IE, Connor JR, Debouck C, Richardson S, Lee Rykaczewski E, Coleman L, Rieman D, Barthlow R, Hastings G, Gowen M 1996 Cathepsin K, but not cathepsins B, L, or S, is abundantly expressed in human osteoclasts. J Biol Chem **271**:12511–12516.
33. Blair HC, Sidonio RF, Friedberg RC, Khan NN, Dong SS 2000 Proteinase expression during differentiation of human osteoclasts in vitro. J Cell Biochem **78**:627–637.
34. Daniell HW, Dunn SR, Ferguson DW, Lomas G, Niazi Z, Stratte PT 2000 Progressive osteoporosis during androgen deprivation therapy for prostate cancer. J Urol **163**:181–186.
35. Ross RW, Small EJ 2002 Osteoporosis in men treated with androgen deprivation therapy for prostate cancer. J Urol **167**:1952–1956.
36. Sinha AA, Gleason DF, DeLeon OF, Wilson MJ, Limas C, Reddy PK, Furcht LT 1991 Localization of type IV collagen in the basement membranes of human prostate and lymph nodes by immunoperoxidase and immuno alkaline phosphatase. Prostate **18**:93–104.
37. Nagle RB, Knox JD, Wolf C, Bowden GT, Cress AE 1994 Adhesion molecules, extracellular matrix, and proteases in prostate carcinoma. J Cell Biochem **19**:232–237.
38. Sinha AA, Gleason DF, Wilson MJ, Staley NA, Furcht LT, Palm SL, Reddy PK, Sibley RK, Martinez-Hernandez A 1989 Immunohistochemical localization of laminin in the basement membranes of normal, hyperplastic, and neoplastic human prostate. Prostate **15**:299–313.
39. Nagle RB, Hao J, Knox JD, Dalkin BL, Clark V, Cress AE 1995 Expression of hemidesmosomal and extracellular matrix proteins by normal and malignant human prostate tissue. Am J Pathol **146**:1498–1507.
40. Burns-Cox N, Avery NC, Gingell JC, Bailey AJ 2001 Changes in collagen metabolism in prostate cancer: a host response that may alter progression. J Urol **166**:1698–1701.
41. Sinha AA, Jamuar MP, Wilson MJ, Rozhin J, Sloane BF 2001 Plasma membrane association of cathepsin B in human prostate cancer: Biochemical and immunogold electron microscopic analysis. Prostate **49**:172–184.
42. Waghray A, Keppler D, Sloane BF, Schuger L, Chen YQ 2002 Analysis of a truncated form of cathepsin H in human prostate tumor cells. J Biol Chem **277**:11533–11538.
43. Fernandez PL, Farre X, Nadal A, Fernandez E, Peiro N, Sloane BF, Shi GP, Chapman HA, Campo E, Cardesa A 2001 Expression of cathepsins B and S in the progression of prostate carcinoma. Int J Cancer **95**:51–55.
44. Friedrich B, Jung K, Lein M, Turk I, Rudolph B, Hampel G, Schnorr D, Loening SA 1999 Cathepsins B, H, L and cysteine protease inhibitors in malignant prostate cell lines, primary cultured prostatic cells and prostatic tissue. Eur J Cancer **35**:138–144.
45. Zhang J, Jung K, Lein M, Kristiansen G, Rudolph B, Hauptmann S, Schnorr D, Loening SA, Lichtinghagen R 2002 Differential expression of matrix metalloproteinases and their tissue inhibitors in human primary cultured prostatic cells and malignant prostate cell lines. Prostate **50**:38–45.
46. Dong Z, Nemeth JA, Cher ML, Palmer KC, Bright RC, Fridman R 2001 Differential regulation of matrix metalloproteinase-9, tissue inhibitor of metalloproteinase-1 (TIMP-1) and TIMP-2 expression in co-cultures of prostate cancer and stromal cells. Int J Cancer **93**:507–515.
47. Berruti A, Dogliotti L, Bitossi R, Fasolis G, Gorzegno G, Bellina M, Torta M, Porpiglia F, Fontana D, Angeli A 2000 Incidence of skeletal complications in patients with bone metastatic prostate cancer and hormone refractory disease: predictive role of bone resorption and formation markers evaluated at baseline. J Urol **164**:1248–1253.
48. Garnero P 2001 Markers of bone turnover in prostate cancer. Cancer Treat Rev **27**:187–192.
49. Lipton A, Costa L, Ali SM, Demers LM 2001 Bone markers in the management of metastatic bone disease. Cancer Treat Rev **27**:181–185.
50. Carter JH, Hugo ER, Holdern T, Porco M, Fritz D 2001 Cysteine protease and cysteine protease inhibitor expression in prostate cancer cell lines. Cancer Res **42**:403.
51. Corey E, Quinn JE, Bladou F, Brown LG, Roudier MP, Brown JM, Buhler KR, Vessella RL 2002 Establishment and characterization of osseous prostate cancer models: Intra-tibial injection of human prostate cancer cells. Prostate **52**:20–33.
52. Yoshida E, Verrusio EN, Mihara H, Oh D, Kwaan HC 1994 Enhancement of the expression of urokinase-type plasminogen activator from PC-3 human prostate cancer cells by thrombin. Cancer Res **54**:3300–3304.
53. Brown JM, Corey E, Lee ZD, True LD, Yun TJ, Tondravi M, Vessella RL 2001 Osteoprotegerin and rank ligand expression in prostate cancer. Urology **57**:611–616.
54. Granchi S, Brocchi S, Bonaccorse L, Baldi E, Vinci MC, Forti G, Serio M, Maggi M 2001 Endothelin-1 production by prostate cancer cell lines is up-regulated by factors involved in cancer progression and down-regulated by androgens. Prostate **49**:267–277.
55. Iwamura M, Abrahamsson PA, Foss KA, Wu G, Cockett AT, Deftos LJ 1994 Parathyroid hormone-related protein: A potential autocrine growth regulator in human prostate cancer cell lines. Urology **43**:675–679.

Address reprint requests to:
Kristen Brubaker, PhD
Department of Urology
University of Washington
Mailstop 356510
1959 NE Pacific St., HSB I-340
Seattle, WA 98195, USA
E-mail: kbrubake@u.washington.edu

Received in original form February 27, 2002; in revised form July 29, 2002; accepted August 16, 2002.

Characterization of C4-2 Prostate Cancer Bone Metastases and Their Response to Castration

Jesco Pfitzenmaier[1,2], Janna E. Quinn[1], Austin M. Odman[1], Jian Zhang[3], Evan T. Keller[3], Robert L. Vessella[1], Eva Corey[1]

1. Department of Urology, University of Washington, Seattle, WA, USA
2. Department of Urology, Johannes Gutenberg-University, Mainz, Germany
3. Department of Pathology, University of Michigan, Ann Arbor, MI, USA

Funding Resources:
CAP CURE, LuCaP Foundation, PO1 CA85859-01A2, Department of the Army reward DAMD17-00-1-0529, and Deutsche Forschungsgemeinschaft (DFG)

Running Title:
C4-2 Prostate Cancer Bone Metastasis Model

Email Addresses of all authors:
jpfitz@gmx.net; jquinn@u.washington.edu; austino@u.washington.edu; jzhang@med.umich.edu; ekeller@med.umich.edu; vessella@u.washington.edu; ecorey@u.washington.edu

JBMR standardized key words: Animal Model, Rodent, Osteoblasts, Bone Densitometry, Bone Histomorphometry

Correspondence:
Eva Corey, Ph.D.
Department of Urology, Mailstop 356510
University of Washington
1959 NE Pacific Street
Seattle, WA 98195, USA
Phone: 206-543-1461
Fax: 206-543-1146
e-mail: ecorey@u.washington.edu

MicroAbstract

New well-characterized pre-clinical models of prostate cancer (CaP) bone metastases are needed to further understanding of the development of CaP-related bone disease in patients. Here we describe characterization of a model consisting of direct injection of C4-2 cells into tibiae.

Abstract

Introduction:

Prostate cancer (CaP) has a high proclivity to metastasize to bone. Development and characterization of pre-clinical models of CaP bone metastases are of high interest. The objective of this study was to characterize C4-2 bone metastases and their response to castration.

Materials and Methods:

Cell suspensions of C4-2, a subline of LNCaP, were injected directly into the tibiae of intact male mice. In groups A (n=7) and B (n=5), animals were sacrificed 3 and 8 weeks after injection of C4-2 cells, respectively. In group C (n=7), animals were castrated 3 weeks after injection, and sacrificed 5 weeks after castration. Serum PSA levels and bone mineral density (BMD) were measured, and bone histomorphometric analysis was performed.

Results:

C4-2 cells decreased BMD of the injected tibiae by 36.1% and bone volume by 74.1% *vs.* normal tibiae. Castration caused a 32.3% drop in serum PSA (p=0.0438), with a nadir at day 14, after which it began to rise again. Bone destruction in the tumorous tibiae of castrated animals was decreased by 15.9% *vs.* tumorous tibiae of intact animals (p=0.0392). However, BMD in the

tumorous tibiae of castrated mice was still lower than in normal tibiae of intact animals. Castration also decreased BMD and bone volume in non-tumorous tibiae ($p=0.0406$, 0.0232, respectively).

Conclusions:

The C4-2 model of bone metastasis recapitulates the response to androgen deprivation observed in CaP patients with bone metastases, and is suitable for study of interactions between tumor and bone cells and evaluation of new therapeutic modalities.

Key words

Prostatic neoplasm; bone; metastasis; models, animal; prostate specific antigen

Introduction

In 2002, approximately 189,000 men in the United States will be diagnosed with prostate cancer (CaP) and nearly 30,200 will die from this disease[1]. Even after primary therapy for localized cancer, such as radical prostatectomy, 15-30% of men will relapse with progressive disease that frequently results in bone metastases[2]. The first line of treatment for recurrent prostate cancer is androgen ablation either by bilateral orchiectomy or by chemical castration[3]. Unfortunately, virtually all recurrent tumors eventually stop responding to hormonal ablation, when upon the disease progresses to clinically significant bone metastases[3]. CaP bone metastases cause osteoblastic and mixed responses in the bone in a high percentage of patients[4-6]. The underlying mechanisms of CaP metastasis, the molecular aspects of the development of androgen independence, and the interactions between CaP cells and their surrounding stromal cells in the bone marrow have not yet been evaluated. Our understanding of processes associated with CaP bone metastases is limited in part because of the paucity of animal models that effectively mimic the human situation. Wang and Stearns[7] developed PC-3 prostate cancer sublines which metastasized to bone, and Shevrin et al.[8,9] established two sublines of the PC-3 cells that colonized bone. Thalmann et al.[4] established a CaP animal model with close similarity to CaP in humans. They used the androgen-dependent, Prostate Specific Antigen (PSA)-producing CaP cell line LNCaP to derive androgen-independent cell lines C4-2 and C4-2B by co-injection of LNCaP cells and human bone marrow stroma fibroblasts. These cells metastasize to murine bone, although at low frequency. However, these and other human CaP metastatic models[10,11] have critical limitations. For example, the C4-2 human CaP models[4,5] are limited by the long time frame between injection of the cancer cells and the appearance of detectable osseous

metastases. PC-3 cells and its sublines result in osteolytic bone lesions, and do not produce PSA, a marker of prostate epithelial cells[12]. To circumvent the low rate of spontaneous metastasis of CaP cells in animal models, we and other have used direct injection of CaP cells into bone[6,12,13].

Herein we report on characterization of a C4-2 model of bone metastasis and its response to castration. C4-2 cells were directly injected into tibiae of intact male SCID mice. Tumor growth was monitored, and changes in bone mineral density and various bone parameters were determined. We also studied the effects of castration on C4-2 bone metastases, bone mineral density, and various bone parameters to describe the consequences of androgen suppression in tumorous and normal bone.

Materials and Methods

Cell Line

C4-2 is a CaP cell line derived from LNCaP cells[4] which grows in the absence of androgens, yet responds to manipulation of androgen levels. Thus it is both "androgen independent" and "androgen sensitive". C4-2 was purchased from Urocore (Oklahoma City, OK) and maintained in RPMI-1640 medium (BioWhittaker, Inc., Walkersville, MD) supplemented with 10% fetal bovine serum (Intergen, Purchase, NY) and 2 mM L-glutamine, under standard culture conditions.

Animal Study

All procedures were performed in compliance with the University of Washington Institutional Animal Care and Use Committee and NIH guidelines. We used four- to six-week old male Fox Chase SCID mice (Charles River, Wilmington, MA). The C4-2 cells (100,000 cells in 10 μl)

were injected into the tibiae as we have described previously[12]. Animals were randomized into 3 groups: group A (n=7) animals were monitored for 8 weeks after injection of C4-2 cells; group B (n=5), animals were monitored for 3 weeks after injection; and group C (n=5), animals were castrated 3 weeks after injection and monitored for an additional 5 weeks. Blood samples were drawn weekly starting two weeks after injection of C4-2 cells. Serum PSA levels were determined by the IMx Total PSA Immunoassay (Abbott Laboratories, Abbott Park, IL). Prior to sacrifice, the animals were anaesthesized and a flat plate radiograph was taken. After sacrifice, the tumorous and contralateral tibiae were harvested.

Bone Mineral Density (BMD)

Bone mineral density was determined by Dual X-ray absorptiometry of the tumorous tibiae and the contralateral tibiae without tumor (group A: n=7, group B: n=5, and group C: n=5). An Eclipse peripheral Dexa Scanner (Norland, Ft. Atkinson, WI) equipped with the company's research software was used. The measurement was performed on a 2.5 mm x 2.5 mm area at the injection site of the tumor cells. The bones were scanned at 2 mm/s with a resolution of 0.1 mm x 0.1 mm. The coefficient of variation (short-term BMD) was less than 3%.

Bone Histomorphometry (BHM)

Tumorous tibiae and contralateral non-tumorous tibiae from group A (n=5), group B (n=5), and group C (n=5) were embedded in methacrylate. Histomorphometry analysis was performed by Skeletech, Inc. 6-μm sections of calcified tibiae stained with Goldner's procedures[14] were used for analysis. Analysis was performed on a region adjacent to the growth plate (0.525-1.225 mm below the growth plate) using the Osteomeasure bone analysis program (Osteometrics, Inc.,

Decatur, GA). The percentages of bone volume and tumor volume in the tissue volume (%BV/TV and %TuV/TV respectively) were calculated. The trabecular thickness in μm (Tb.Th), the trabecular number per mm (Tb.N), the trabecular separation in μm (Tb.Sp), the ratio of osteoblast surface to bone surface as a percentage (Ob.S/BS), and the ratio of osteoclast surface to bone surface as a percentage (Oc.S/BS) were also determined. Osteoclasts were visualized by staining for TRAP activity using a leukocyte acid phosphatase kit (Sigma Chemical Company, St. Louis, MO).

Statistical Analysis

Prism GraphPad 3.0 software (GraphPad Software, San Diego, CA) was used to perform statistical analyses. The significance of differences in BMD values and bone histomorphometry parameters was tested using paired and unpaired Student's t-tests as appropriate. The significance of differences in the serum PSA levels was tested using one-way ANOVA. The statistical significance level used was $p \leq 0.05$

Detection of Androgen Receptor(AR)

RT-PCR was performed to confirm expression of AR in C4-2 cells used for these experiments. RNA was extracted using STAT 60 (Tel-test, Inc., Friendswood, TX) as recommended by the manufacturer and 1 μg of total RNA was reverse transcribed using the 1st-Strand™ cDNA synthesis kit (Clontech, Palo Alto, CA). PCR was performed using 2 μl of cDNA and primers AR5: TGA GTA CCG CAT GCA CAA GTC C, and AR 3: CCT GGC TTC CGC AAC TTA CAC using a two-step procedure with the following conditions: 3 min at 80°C for 1 cycle, 5 sec

at 95°C, 1 min at 65°C for 30 cycles, and 7 min at 72°C for 1 cycle. Immunohistochemistry was used to detect AR protein. Immunohistochemical staining was performed on 5-μm sections using standard immunoperoxidase staining techniques on paraffin-embedded sections with an anti-human androgen receptor monoclonal antibody (F39.4.1, BioGenex, San Ramon, CA, 1:50, 1 hour at room temperature, standard antigen retrieval in 10 mM citrate buffer, pH=6). Negative controls were run under the same conditions except that primary antibodies were replaced with MOPC-21 (an unrelated IgG_1 monoclonal antibody), at the same concentration. Immunoreactivity was detected using biotinylated anti-mouse antibodies and an ABC kit (Vector Laboratories, Burlingame, CA), with DAB as substrate.

Results

The take rate of C4-2 cells injected into the proximal end of the tibiae was 100% in all groups (group A: 7/7; group B: 5/5; group C: 5/5). Representative examples of radiographs and histology of tumorous tibiae are shown in Figure 1 and 2, respectively. We first confirmed expression of the AR message and protein. We detected AR messages in C4-2 cells grown *in vitro* and AR protein was detected by immunohistochemistry in C4-2 subcutaneous tumors as well as in C4-2 tumors grown in tibiae (Figure 3A). Serum PSA levels showed no statistically significant differences among the 3 groups during the first 3 weeks (at day 14: $p=0.4239$; at day 21: $p=0.5374$; one-way ANOVA). Serum PSA levels 3 weeks after injection of C4-2 cells were 8.02 ± 1.67 ng/ml. PSA levels rose thereafter in group A, intact animals, until sacrifice (Figure 3 B). Animals in group B were sacrificed at 3 weeks to obtain control values of tumor and bone parameters before castration. PSA serum levels in group C decreased after castration, reaching a

nadir 2 weeks post-castration (35 days after injection of C4-2 cells). The levels declined to 67.7% of the serum levels measured at the time of the castration (p=0.0438; paired t-test). Serum PSA levels were significantly lower in group C than in group A between day 28 and day 49 (day 28: p= 0.0306; day 35: p=0.0074; day 42: p=0.0037; day 49: p=0.0140; unpaired t-test). As seen in prostate cancer patients at the hormone-refractory stage, serum PSA levels began to rise again in group C at day 56 until significant differences between intact (group A) and castrated (group C) animals were no longer seen (p=0.3023; unpaired t-test).

Bone Mineral Density

Changes in bone mineral density (BMD) of tibiae of animals with C4-2 cells in the bone and representative scans of tibiae are presented in Figure 4. C4-2 cells present in tibiae for 3 weeks (group B) decreased BMD *vs.* non-tumorous tibiae (NT) in group B by 15.1%, but these changes did not reach significance (p=0.1100). Tumorous tibiae (TT) of animals in group A exhibited 36.1% lower BMD *vs.* NT of animals in group A (p=0.0005) and 28.4% lower BMD *vs.* TT in group B (p=0.0005). BMD of NT in groups A and B was not different (p=0.8531), indicating that the bone was fully developed when castration was performed. BMD in TT of group C (castrated animals) measured at the end of the experiment (8 weeks) was 15.9% higher than in TT of group A (intact animals; p=0.0392). However there was a 9.6% decrease in BMD in NT in castrated mice (group C) *vs.* NT of intact animals (group A, p=0.0406).

Bone Histomorphometry

Bone histomorphometry results are summarized in Table 1. The analysis of the bone response to prostate tumor cells and androgen ablation did not include the growth plate, where the bone

remodelling could have been affected by the injection (mechanical injury). Since the area proximal to the growth plate was not included in the analysis, we believe that the changes in bone parameters after injection of C4-2 prostate cancer cells reported are not attributable to the injection but to the tumor growth and factors expressed by C4-2 prostate cancer tumor cells; however, we plan to include a sham-injection control group in future studies. In this work the contralateral tibiae that were not injected were used as control samples. C4-2 cells filled ~54% of TV of the evaluated area by 3 weeks after injection, with a further increase in %TuV/TV by week 8. Castration significantly hindered tumor growth; there were no significant increases in %TuV/TV between groups B and C ($p=0.4322$; unpaired t-test), and %TuV/TV was significantly lower in group C *vs.* group A ($p=0.0094$). At 3 weeks after injection of C4-2 cells into tibiae, when %TuV/Tv was already ~54%, we detected no significant changes in %BV/TV, Tb.Th, Tb.Sp, or Tb.N. in TT *vs.* NT. However, the Ob.S/BS and OcS/Bs were already increased. When C4-2 cells were present in the bone environment for 8 weeks (group A), they caused significant decreases in %BV/TV ($p=0.0129$) and trabecular number ($p=0.0042$), but not trabecular thickness ($p=0.2702$). C4-2 cells in the bone environment significantly increased Ob.S/BS and Oc.S/BS ($p=0.0370$ and $p=0.0234$ respectively), suggesting stimulation of bone remodelling. No differences were seen between the NT of untreated animals after 3 and 8 weeks ($p=0.7898$; unpaired t-test). Castration abolished loss of %BV/TV caused by C4-2 cells in 3 out of 5 animals. We detected no significant differences in %BV/TV between TT of these 3 animals and NT in group A or group B ($p=0.8013$ and 0.9964, respectively). %BV/TV of the 3 animals was higher than in TT of intact animals in group A ($p=0.0026$). Moreover, as in the human situation, androgen ablation decreased %BV/TV in the NT *vs.* NT of intact mice by 48.7% ($p=0.0232$). We

performed analysis of correlations between serum PSA levels and the BMD, %TuV/TV, and other parameters measured by histomorphometry, and detected no significant correlations.

Discussion

Advanced CaP patients with lymph-node and bone metastases are treated with androgen suppression induced by either surgical or pharmacological castration, but in the end stage of the disease, patients almost invariably develop hormone-refractory CaP. The phenotypic changes in the cancer cells accompanying the development of androgen independence and the effects of these changes on their interactions with the bone environment are not well understood. Insight into these processes could help to identify key factors and "pressure points" for therapy. Animal models that mimic the human disease are critical for elucidation of the alterations in both tumor and bone cells and evaluation of new therapeutics.

Herein we describe the use of the C4-2 CaP cell line in direct intra-tibial injections to study the responses of CaP cells to androgen ablation and examine the effects on interactions of CaP and bone cells. CaP–osseous models employing direct injection that have been characterized to date have various limitations: androgen-dependent LAPC9 and LuCaP 23.1, which result in osteoblastic lesions, do not grow *in vitro*; androgen-sensitive LNCaP, which results in mixed lesions, has a low take rate and a rather slow growth rate in the tibiae; and androgen-insensitive PC-3 cells, which do not express PSA, result in osteolytic lesions. The use of C4-2 cells addresses some of these limitations, since C4-2 cells express PSA and the androgen receptor, grow in the absence of androgens but still respond to androgens, and also grow *in vitro* and are therefore susceptible to genetic manipulations. There are therefore several aspects of the C4-2

model which successfully mimic characteristics of human tumors. However, our detailed bone histomorphometric analysis of C4-2 bone metastases clearly shows that C4-2 cells result in overall decreases in bone volume and bone mineral density, and therefore do not yield predominantly osteoblastic reaction in bone, as observed in ~90% of CaP patients. Nevertheless, C4-2 cells stimulated bone remodeling, as demonstrated by increased numbers of both osteoblasts and osteoclasts. Thus the most accurate description of C4-2 bone metastases is that they are mixed lesions, with net decrease in bone mineral density and bone volume. Our evaluation of human bone metastases has shown that both mixed and lytic lesions are also present in CaP patients, including those exhibiting overall blastic character[15].

C4-2 cells exhibited a high take rate (100%) and a consistent growth rate in the intra-tibial injections. C4-2 tumors were detectable after 3 weeks in all animals by serum PSA levels, and at that time %TuV/TV was ~54% as determined by histomorphometry analysis. Interestingly, when we examined effects of C4-2 cells on bone at an early time point, 3 weeks after injection of C4-2 cells, we detected a decrease of only ~10% in BMD, which did not reach significance, and there were no significant changes in %BV/TV. We hypothesize that large numbers of tumor cells are required to dysregulate the bone-remodelling equilibrium or that the perturbations require more time to be observable. Longer exposure of bone to the C4-2 cells and increased %TuV/TV resulted in a significant decrease in BMD and in %BV/TV. These results are in agreement with results previously reported with C4-2B cells[16].

Serum PSA levels rose consistently in the intact animals from week 2 until the end of the experiment, closely tracking the tumor volume. Androgen suppression caused a decrease in

serum PSA levels, with a nadir at 2 weeks post-castration, after which serum PSA levels began to rise again. This is similar to the course observed in humans as metastatic prostate cancer reaches the hormone-refractory stage. It is interesting to note that serum PSA levels were not significantly different between intact and castrated animals at the end of the study, but the %TuV/TV was significantly lower in the castrated animals. This fact may be explained by changes in the mechanisms of regulation of PSA expression. In the intact animals PSA is regulated by testosterone, as is growth of prostate cancer cells, and therefore PSA levels follow tumor volume. After androgen ablation, however, when tumors begin to grow in an androgen-independent manner, other mechanisms activate the androgen receptor and regulate PSA, and still other mechanisms may be involved in growth regulation. Under these conditions PSA does not reliably track tumor volume, as has been reported in clinical situations with hormone-independent CaP[17].

Growth of C4-2 bone metastases was also inhibited by androgen suppression. We detected decreased levels of PSA and decreased %TuV/TV in TT of castrated animals *vs.* intact animals. Moreover, in 3 out of 5 animals, androgen ablation halted bone lysis associated with C4-2 cells in the tibiae; despite the presence of tumor cells in the bone, %BV/TV in TT and NT in castrated animals was the same.

Our results also demonstrated that androgen ablation decreases BMD and %BV/TV in NT. The C4-2–osseous model therefore mimics the human situation, in which an osteoporotic response to androgen suppression is seen not only in the tumor but in the whole skeleton[18]. Evidently the

model can be used to study both the interactions of CaP cells with the bone and the effects of androgen suppression on CaP bone metastasis.

In conclusion, we have established and characterized the C4-2 model of CaP bone metastasis and its response to androgen ablation. Our results show that the C4-2–osseous model exhibits many aspects of bone metastases of advanced prostate cancer in patients, although it does not possess the overall osteoblastic character (increase in bone volume) which is the hallmark of CaP bone metastases in patients with advanced disease. However, bone resorption is believed to be an essential component in the establishment of bone metastases. Therefore, models demonstrating both bone resorption and formation can provide useful information related to perturbation of normal bone remodelling by CaP bone metastases. This is the first detailed characterization of the response of bone to CaP metastases with mixed blastic/lytic character and the effects of androgen ablation on these metastases. The model should be useful in studying the interactions between prostate cancer cells and the bone environment and evaluating new therapeutic modalities for treatment of CaP bone metastases.

Acknowledgement

We would like to thank Dr. Michael Corey for his editorial help and Abbott Laboratories for providing reagents for PSA determinations. This work was supported by the LuCaP Foundation, PO1 CA85859-01A2, CAP CURE, and the Deutsche Forschungsgemeinschaft (DFG).

To whom reprint requests should be addressed:

Eva Corey, Ph.D.; Department of Urology; University of Washington; Mailstop 356510; 1959 NE Pacific Street; Seattle, WA 98195; USA; Phone: 206-543-1461; Fax: 206-543-1146; e-mail: ecorey@u.washington.edu

Manufacture's names: Charles River, Urocore, BioWhitaker, Intergen, Abbott Laboratories, Tel-test, Inc, Clontech, BioGenex, Vector Laboratories, Norland, Skeletech, Sigma, Osteometrics, GraphPad Software.

References:

1. Jemal A, Thomas A, Murray T, Thun M 2002 Cancer statistics, 2002. CA Cancer J Clin **52:**23-47.

2. Rigaud J, Tiguert R, Le Normand L, Karam G, Glemain P, Buzelin JM,Bouchot O 2002 Prognostic value of bone scan in patients with metastatic prostate cancer treated initially with androgen deprivation therapy. J Urol **168:**1423-1426.

3. Oefelein MG, Ricchiuti VS, Conrad PW, Goldman H, Bodner D, Resnick MI,Seftel A 2002 Clinical predictors of androgen-independent prostate cancer and survival in the prostate-specific antigen era. Urology **60:**120-124.

4. Thalmann GN, Anezinis PE, Chang SM, Zhau HE, Kim EE, Hopwood VL, Pathak S, von Eschenbach AC,Chung LW 1994 Androgen-independent cancer progression and bone metastasis in the LNCaP model of human prostate cancer. Cancer Res **54:**2577-2581.

5. Thalmann GN, Sikes RA, Wu TT, Degeorges A, Chang SM, Ozen M, Pathak S,Chung LW 2000 LNCaP progression model of human prostate cancer: androgen-independence and osseous metastasis. Prostate **44:**91-103.

6. Wu TT, Sikes RA, Cui Q, Thalmann GN, Kao C, Murphy CF, Yang H, Zhau HE, Balian G,Chung LW 1998 Establishing human prostate cancer cell xenografts in bone: induction of osteoblastic reaction by prostate-specific antigen-producing tumors in athymic and SCID/bg mice using LNCaP and lineage-derived metastatic sublines. Int J Cancer **77:**887-894.

7. Wang M and Stearns ME 1991 Isolation and characterization of PC-3 human prostatic tumor sublines which preferentially metastasize to select organs in S.C.I.D. mice. Differentiation **48:**115-125.

8. Shevrin DH, Kukreja SC, Ghosh L,Lad TE 1988 Development of skeletal metastasis by human prostate cancer in athymic nude mice. Clin Exp Metastasis **6:**401-409.

9. Shevrin DH, Gorny KI,Kukreja SC 1989 Patterns of metastasis by the human prostate cancer cell line PC-3 in athymic nude mice. Prostate **15:**187-194.

10. Klein KA, Reiter RE, Redula J, Moradi H, Zhu XL, Brothman AR, Lamb DJ, Marcelli M, Belldegrun A, Witte ON,Sawyers CL 1997 Progression of metastatic human prostate cancer to androgen independence in immunodeficient SCID mice. Nat Med **3:**402-408.

11. Berlin O, Samid D, Donthineni-Rao R, Akeson W, Amiel D,Woods VL, Jr. 1993 Development of a novel spontaneous metastasis model of human osteosarcoma transplanted orthotopically into bone of athymic mice. Cancer Res **53:**4890-4895.

12. Corey E, Quinn JE, Bladou F, Brown LG, Roudier MP, Brown JM, Buhler KR,Vessella RL 2002 Establishment and characterization of osseous prostate cancer models: intra-tibial injection of human prostate cancer cells. Prostate **52:**20-33.

13. Nemeth JA, Harb JF, Barroso U, Jr., He Z, Grignon DJ,Cher ML 1999 Severe combined immunodeficient-hu model of human prostate cancer metastasis to human bone. Cancer Res **59:**1987-1993.

14. Villanueva AR and Mehr LA 1977 Modifications of the Goldner and Gomori one-step trichrome stains for plastic-embedded thin sections of bone. Am J Med Technol **43:**536-538

15. Roudier MP, Sherrard DJ, True LD, Ott-Ralph SM, Meligro C, Berrie M, Soo CCY, Felise DG, Quinn JE, Vessella R 2000 Heterogeneous bone histomorphometric patterns in metastatic prostate cancer. J Bone Miner Res **15:** S567 (abstract).

16. Zhang J, Dai J, Qi Y, Lin DL, Smith P, Strayhorn C, Mizokami A, Fu Z, Westman J,Keller ET 2001 Osteoprotegerin inhibits prostate cancer-induced osteoclastogenesis and prevents prostate tumor growth in the bone. J Clin Invest **107:**1235-1244.

17. Harris KA, Weinberg V, Bok RA, Kakefuda M,Small EJ 2002 Low dose ketoconazole with replacement doses of hydrocortisone in patients with progressive androgen independent prostate cancer. J Urol **168:**542-545.

18. Oefelein MG, Ricchuiti V, Conrad W, Seftel A, Bodner D, Goldman H,Resnick M 2001 Skeletal fracture associated with androgen suppression induced osteoporosis: the clinical incidence and risk factors for patients with prostate cancer. J Urol **166:**1724-1728.

Table 1.

		Group A	Group B	Group C
Tumor volume (TuV/TV; %)	**TT**	83.75 ± 2.90	53.61 ± 20.83	67.16 ± 3.94
Trabecular bone volume (BV/TV; %)	**TT**	2.69 ± 0.44	9.10 ± 4.56	6.38 ± 2.24
	NT	10.40 ± 1.85	9.68 ± 1.09	5.06 ± 0.47
Trabecular number (Tb.N; #/mm^2)	**TT**	0.95 ± 0.21	2.57 ± 1.13	2.06 ± 0.63
	NT	2.89 ± 0.37	2.85 ± 0.31	1.35 ± 0.10
Trabecular thickness (Tb.Th; μm)	**TT**	30.53 ± 3.11	32.63 ± 3.82	28.46 ± 2.09
	NT	35.46 ± 3.12	33.94 ± 1.12	37.77 ± 2.80
Trabecular separation (Tb.Sp; μm)	**TT**	1322.00 ± 375.90	995.20 ± 751.00	849.00 ± 335.20
	NT	344.90 ± 68.41	325.80 ± 41.75	721.50 ± 58.43
Osteoblast surface (Ob.S/BS; %)	**TT**	7.84 ± 2.50	7.80 ± 1.81	10.07 ± 4.17
	NT	0.12 ± 0.12	2.05 ± 2.05	0.75 ± 0.34
Osteoclast surface (Oc.S/BS; %)	**TT**	12.49 ± 2.39	10.06 ± 6.06	7.11 ± 1.63
	NT	2.73 ± 0.54	3.72 ± 0.18	3.63 ± 1.66

Table 1: Results for bone histomorphometry are shown as mean ± SEM for group A (C4-2, 8 weeks), group B (C4-2, 3 weeks), and group C (C4-2, castrated, 8 weeks). *TT* tibiae with tumor; *NT* tibiae without tumor; *TuV* tumor volume; *TV* tissue volume; *BV* bone volume; *Tb.N* trabecular number; *Tb.Th* trabecular thickness; *Tb.Sp* trabecular separation; *Ob.S* osteoblast surface; *BS* bone surface; *Oc.S* osteoclast surface.

Figure 1. Radiographs of C4-2 Bone Metastases.

A: normal tibia; B: tibia with C4-2 tumor 3 weeks after injection of C4-2 cells; C: tibia with C4-2 tumor 8 weeks after injection of C4-2 cells; D and E: tibiae with C4-2 tumors 5 weeks after castration.

Figure 2. Histological Appearance of C4-2 Metastases.

Calcified tibiae were stained with Goldner's stain. Normal tibia after 8 weeks is shown in A. After 3 weeks the tumor starts to grow in the bone (B). C4-2 cells replace all bone marrow by week 8 (C) and cause destruction of mineralized bone. Androgen ablation inhibited bone destruction in 3 animals (D), but in the other 2 animals (E) the bone destruction was similar to that observed in intact animals. Mineralized bone is presented by *green* area; tumor cells are *grey*.

Figure 3.

A. Expression of Androgen Receptor in C4-2 Cells.

(A) AR messages were detected in C4-2 cells grown in tissue culture. AR protein was detected in nuclei of C4-2 cells grown in subcutaneous tumors (B) and C4-2 intra-tibial tumors (C) by immunohistochemistry as described in the Methods section.

B. Serum PSA Levels Post-intra-tibial C4-2-Injections.

The levels are plotted as mean ± SEM. Group A: mice were sacrificed on day 56; group C: mice were castrated at day 21 and sacrificed on day 56. Serum PSA levels were not different on day

14, 21, and 56, but differed on day 28, 35, 42, and 49, as indicated by '[a]'. *PSA* prostate specific antigen.

Figure 4. Changes in Bone Mineral Density in C4-2 Bone Metastases.

Measurement of bone mineral density (BMD) was performed by Dual X-ray absorptiometry. **A.** Representative scans of groups A, B, and C are shown. **B.** Values are normalized to group A (NT) and are plotted as mean ± SEM. An increasing loss of BMD caused by the tumor can be seen between 3 weeks (group B (TT)) and 8 weeks (group A (TT)). Androgen suppression prevented extensive bone loss in the tumor-bearing tibiae (group A (TT) *vs.* group C (TT)). In contrast, a decrease in BMD was detected in NT of castrated animals (group C) *vs.* NT of intact animals (group A). *BMD* bone mineral density; *TT* tibia with tumor; *NT* tibia without tumor.

Figure 5.

A. %TuV/TV in Tibiae with and without C4-2 Bone Metastases in Intact and Castrated Animals. Tumor volume was measured on calcified samples stained by Goldner's stain using Osteomeasure software as described in Methods Section. The values are plotted as mean ± SEM. Castration decreased the tumor growth (group A *vs.* group C), but did not entirely prevent expansion of the tumor (group B *vs.* group C). *TuV* tumor volume; *TV* tissue volume.

B. %BV/TV in Tibiae with and without C4-2 Bone Metastases in Intact and Castrated Animals. Values are normalized to group A (NT) and are plotted as mean ± SEM. The response to the tumor in intact animals (group A (TT)) was osteolytic, but the response in castrated

animals resulted in a higher proportion of bone (group C (TT)). *BV* bone volume; *TT* tibia with tumor; *NT* tibia without tumor.

FIGURE 1

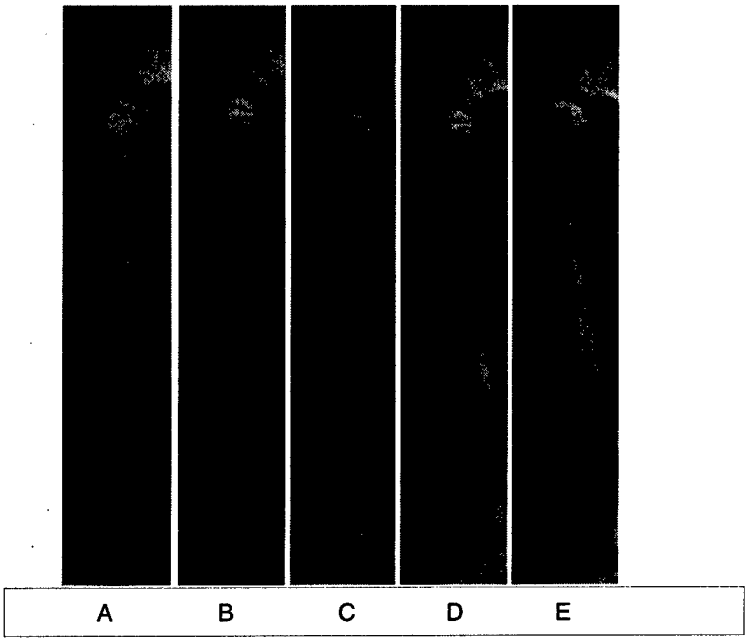

FIGURE 2

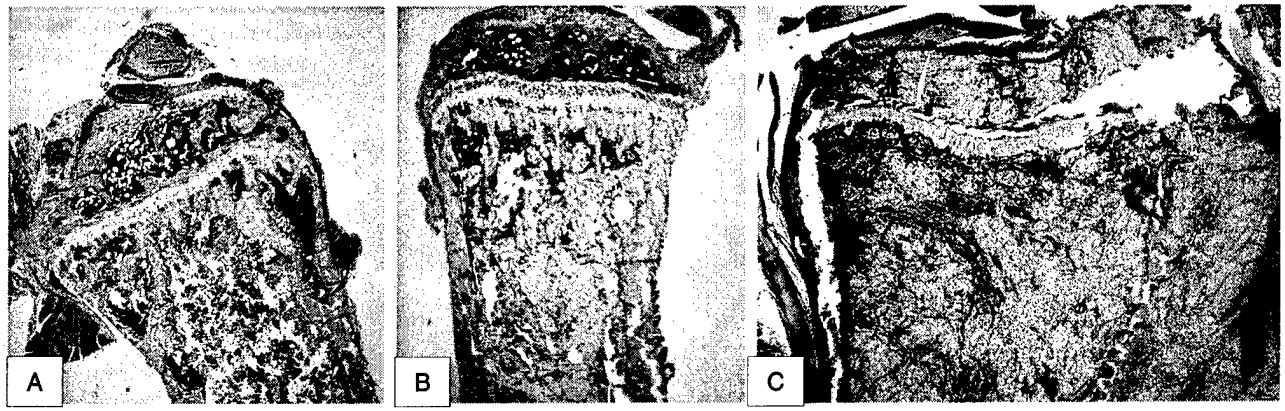

NORMAL TIBIA

C4-2 TUMORED TIBIA
(3 WEEKS)

C4-2 TUMORED TIBIA
(8 WEEKS)

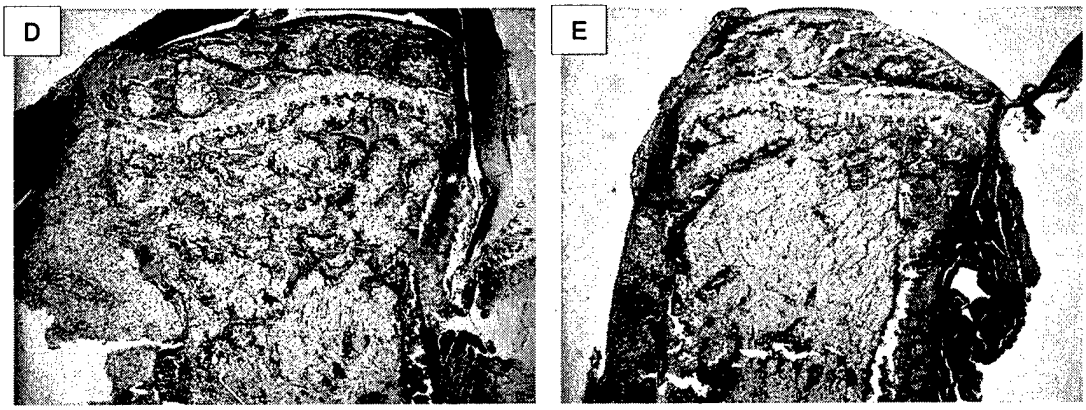

C4-2 TUMOROUS TIBIAS AFTER CASTRATION

FIGURE 3

A

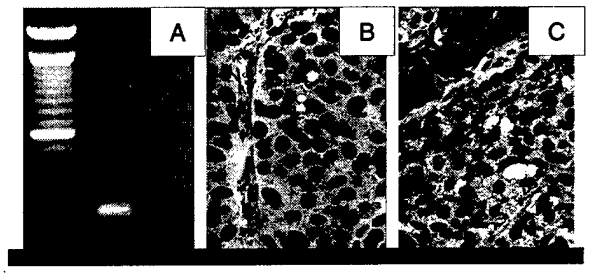
A
B
C

B

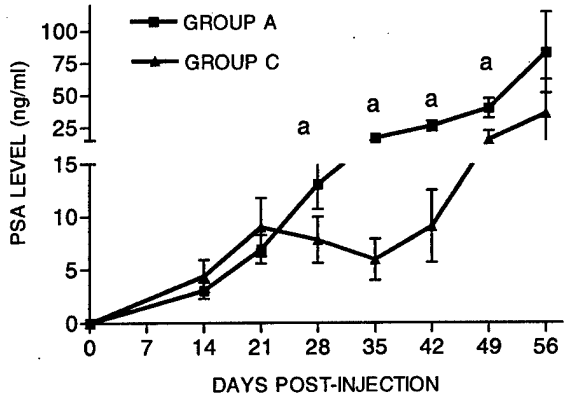
GROUP A
GROUP C
PSA LEVEL (ng/ml)
100
75
50
25
15
10
5
0
a
a
a
a
0
7
14
21
28
35
42
49
56
DAYS POST-INJECTION

FIGURE 4

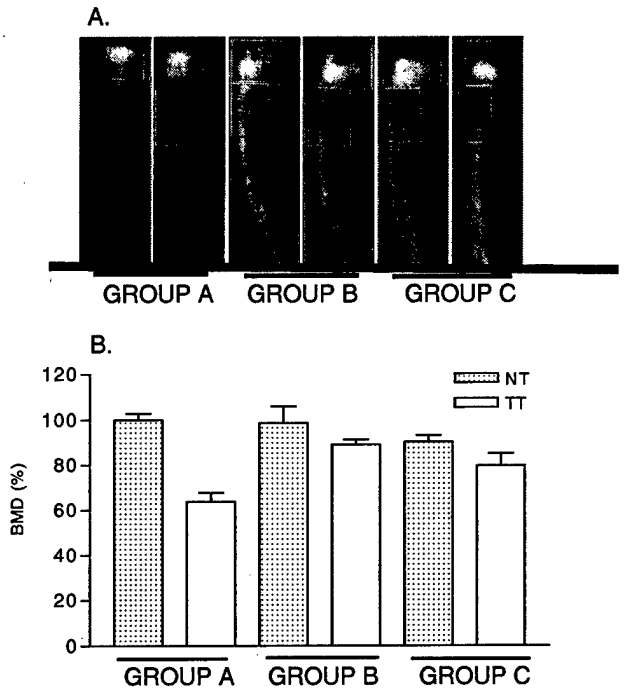
A.
GROUP A
GROUP B
GROUP C
B.
NT
TT
BMD (%)
120
100
80
60
40
20
0
GROUP A
GROUP B
GROUP C

FIGURE 5

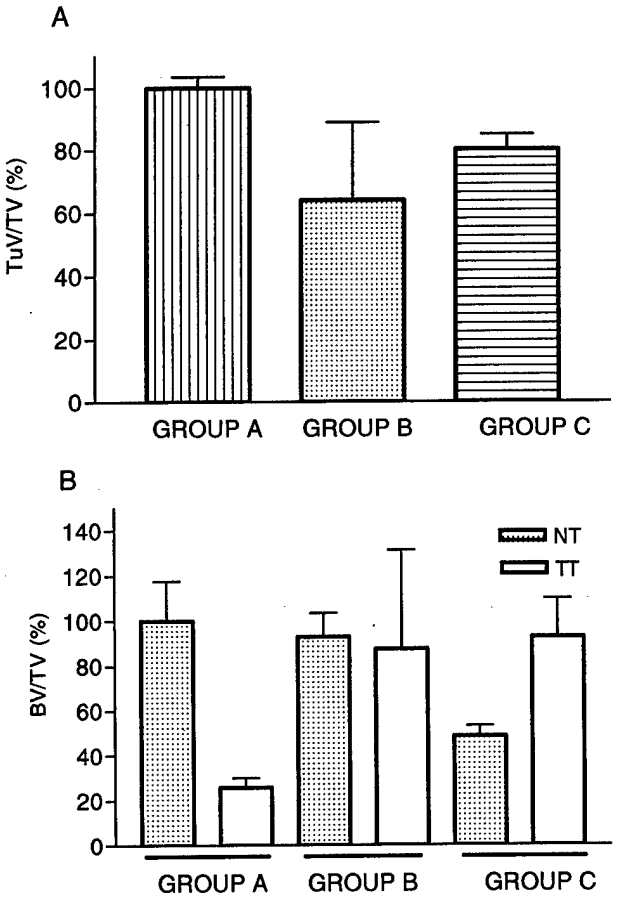
A
TuV/TV (%)
100
80
60
40
20
0
GROUP A
GROUP B
GROUP C
B
BV/TV (%)
140
120
100
80
60
40
20
0
NT
TT
GROUP A
GROUP B
GROUP C